PAPER • OPEN ACCESS

A thermodynamically consistent Markovian master equation beyond the secular approximation

To cite this article: Patrick P Potts *et al* 2021 *New J. Phys.* **23** 123013

View the article online for updates and enhancements.

New Journal of Physics

The open access journal at the forefront of physics

PAPER

A thermodynamically consistent Markovian master equation beyond the secular approximation

Patrick P Potts[1,2,*] , Alex Arash Sand Kalaee[1] and Andreas Wacker[1]

1   Physics Department and NanoLund, Lund University, Box 118, 22100 Lund, Sweden
2   Department of Physics, University of Basel, Klingelbergstrasse 82, 4056 Basel, Switzerland
*   Author to whom any correspondence should be addressed.

E-mail: patrick.potts@unibas.ch

Abstract

Markovian master equations provide a versatile tool for describing open quantum systems when memory effects of the environment may be neglected. As these equations are of an approximate nature, they often do not respect the laws of thermodynamics when no secular approximation is performed in their derivation. Here we introduce a Markovian master equation that is thermodynamically consistent and provides an accurate description whenever memory effects can be neglected. The thermodynamic consistency is obtained through a rescaled Hamiltonian for the thermodynamic bookkeeping, exploiting the fact that a Markovian description implies a limited resolution for heat. Our results enable a thermodynamically consistent description of a variety of systems where the secular approximation breaks down.

1. Introduction

Theoretical descriptions of open quantum systems are crucial for understanding various scenarios, as a complete shielding from the environment is usually not feasible or not even desirable. The latter is the case in the field of quantum thermodynamics, where heat flows in out-of-equilibrium situations are the key issue of concern. As a microscopic description of the environmental degrees of freedom becomes quickly intractable, numerous approaches exist to approximate the behavior of the degrees of freedom of the system alone [1–4]. Of particular interest are Markovian master equations in so-called GKLS form, after Gorini *et al* [5], and Linblad [6]. By neglecting any memory effects induced by the environment, they provide a particularly tractable description that gives access to the full density matrix of the system alone (i.e. the reduced system). These equations usually rely on Born–Markov approximations which do not ensure GKLS form. For this reason additional approximations are usually employed.

The most prominent approximation is the so-called secular approximation [1], where oscillating terms are dropped from the master equation (for a recent generalization to time-dependent systems, see reference [7]). This approximation has the desirable feature that it ensures consistency with the laws of thermodynamics. The secular approximation has also been termed the *global* approach, because it uses the (delocalized) eigenstates of the Hamiltonian. This is in contrast to the *local* approach which is widely used in, e.g. quantum optics [8, 9] (for a comparison between the global and the local approach, see references [10–20]). The difference between the local and the global approach becomes particularly apparent when considering a system of weakly coupled components (e.g. two or three qubits or harmonic oscillators weakly coupled to each other). In this case, the local approach can be obtained by deriving a master equation for the individual, uncoupled components and simply adding the coupling term. We stress however that the local approach is by no means phenomenological, as a microscopic derivation exists [13, 20]. This approach is appealing mainly for two reasons: first, it does not require diagonalization of the Hamiltonian and can thus be applied to problems where a secular approximation is difficult to implement analytically. Second, it holds for systems that consist of weakly coupled degenerate units, where the secular approximation breaks

down due to the near-degeneracies. Such systems are widely studied in the field of quantum thermodynamics as they are promising for manipulating and exploiting heat flows [21, 22]. However, the local approach was criticized for not being thermodynamically consistent as it may result in violations of the second law of thermodynamics [23]. These violations where shown to be small as long as the local approach is justified [24, 25]. One may thus argue that sizable violations of the second law provide a useful *red flag*, indicating that the approach is applied outside its regime of validity. Nevertheless, thermodynamic consistency is desirable in any Markovian master equation as it allows for falling back on well established laws [26]. It was shown that the local approach can be rendered thermodynamically consistent by re-defining heat. This was motivated from a collisional model, where work is required to maintain the collisions [27], as well as directly from the master equation itself [28]. Below, we show how thermodynamic consistency of the local approach can be obtained starting from the standard microscopic system-bath picture by exploiting a crucial insight: *the approximations that result in a Markovian master equation impose limitations on the energy-resolution for heat*. Within this limited resolution, we may re-define heat without compromising the accuracy of the approach.

Recently, a novel approach termed PERLind (position and energy resolved Lindblad equation) was introduced [29] in an attempt to interpolate between the local and global approach. Since then, multiple microscopic derivations were given [30–33], showing that the PERLind approach does not require any additional assumptions going beyond the ones already present when performing Born–Markov approximations. Compared to the global and local approaches, the PERLind approach thus has an increased regime of validity, making it a very promising approach. However, it also comes with disadvantages: it requires diagonalization of the Hamiltonian and it is not thermodynamically consistent. Furthermore, an analytical treatment is often complicated by tedious expressions as shown below. Another approach that goes beyond the secular approximation is based on introducing a coarse-graining time [15, 34–38]. While taking this time to infinity recovers the global master equation, a GKLS master equation can be obtained by choosing a finite coarse-graining time. In general, coarse-grained master equations are not thermodynamically consistent. However, just as for the local approach, thermodynamic consistency can be recovered by re-defining heat as motivated by a collisional model [39]. Yet an alternative approach for obtaining a GKLS master equation beyond the secular approximation is provided by truncating the Redfield equation [40].
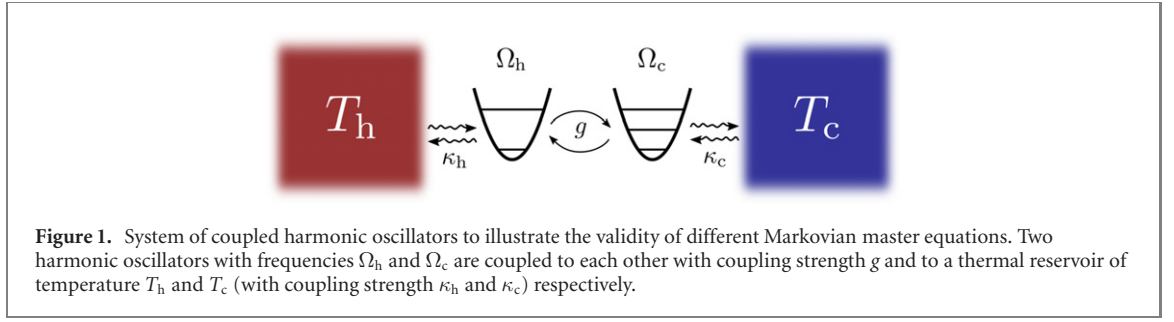
Here we introduce a novel Markovian master equation in GKLS form that goes beyond the secular approximation. Its main merit compared to previous approaches is that it is thermodynamically consistent. Our approach is based on the same principle that is at the heart of all Markovian master equations: the environment properties are slowly changing in energy. This allows us to not only neglect the broadening of energy levels but to also treat transition energies that are close as having the same value. Employing the same approximation in the definition of heat then naturally results in a thermodynamically consistent treatment. Our approach may reduce to the global approach (when no transition energies are close) or to a thermodynamically consistent version of the local approach (when all transition energies are close). We note that for a time-independent Hamiltonian, our results are in agreement with the *unified GKLS master equation* which was very recently derived in an independent work [41].

The rest of this paper is structured as follows. In section 2, we compare different Markovian master equations and illustrate the main results without going into technical details. In particular, we introduce a thermodynamically consistent local master equation as an example of our general master equation, which is derived in section 3. Sections 4 and 5 illustrate our master equation with the examples of a fermionic and a bosonic heat engine, covering both the time-independent as well as the time-dependent case. In section 6, we apply our master equation to an interacting double quantum dot, a problem where we do not have an exact solution and where our master equation may provide a description that differs from both the global and the local approach. We conclude in section 7.

2. Comparing different master equations

In this section, we compare different master equations, in order to illustrate some of our main results without going into mathematical details. To shed light on the discussion about the thermodynamic consistency, we focus on the system that was considered in reference [23], where it was shown that a local approach (here referred to as *conventional local* approach) may violate the second law of thermodynamics. The system (sketched in figure 1) consists of two coupled harmonic oscillators and is described by the Hamiltonian

$$\hat{H}_\mathrm{S} = \Omega_\mathrm{c}\hat{a}_\mathrm{c}^\dagger\hat{a}_\mathrm{c} + \Omega_\mathrm{h}\hat{a}_\mathrm{h}^\dagger\hat{a}_\mathrm{h} + g(\hat{a}_\mathrm{h}^\dagger\hat{a}_\mathrm{c} + \hat{a}_\mathrm{c}^\dagger\hat{a}_\mathrm{h}) = \Omega_+\hat{a}_+^\dagger\hat{a}_+ + \Omega_-\hat{a}_-^\dagger\hat{a}_-, \qquad (1)$$

Figure 1. System of coupled harmonic oscillators to illustrate the validity of different Markovian master equations. Two harmonic oscillators with frequencies Ω_h and Ω_c are coupled to each other with coupling strength g and to a thermal reservoir of temperature T_h and T_c (with coupling strength κ_h and κ_c) respectively.

with the standard commutation relations

$$[\hat{a}_\alpha, \hat{a}_\beta^\dagger] = \delta_{\alpha,\beta}, \qquad [\hat{a}_\alpha, \hat{a}_\beta] = 0. \tag{2}$$

The two oscillators are labeled by c and h, as they are coupled to a cold and a hot bath respectively. Diagonalizing the Hamiltonian results in the eigenfrequencies

$$\Omega_\pm = \bar{\Omega} \pm \sqrt{\Delta^2 + g^2}, \quad \bar{\Omega} = \frac{\Omega_c + \Omega_h}{2}, \quad \Delta = \frac{\Omega_h - \Omega_c}{2}, \tag{3}$$

and the corresponding ladder operators

$$\hat{a}_+ = \cos(\theta/2)\hat{a}_h + \sin(\theta/2)\hat{a}_c, \qquad \hat{a}_- = -\sin(\theta/2)\hat{a}_h + \cos(\theta/2)\hat{a}_c, \tag{4}$$

where the angle θ is defined through

$$\cos(\theta) = \frac{\Delta}{\sqrt{\Delta^2 + g^2}}, \tag{5}$$

where we use the branch $0 \leqslant \theta \leqslant \pi$, which corresponds to $g > 0$, which we tacitly assume throughout this work.

We will now compare five different approaches to describe the heat transport through this system:

(a) The transmission function approach (valid for arbitrary system-bath coupling).
(b) The conventional local approach (may violate the second law of thermodynamics).
(c) Our local approach (ensures the laws of thermodynamics).
(d) The global approach (relies on the secular approximation).
(e) The PERLind approach (interpolates between local and global).

As we show below, the master equation we introduce in this work reduces either to the local, or to the global approach depending on the parameters. We stress that the approach we refer to as *local* is thermodynamically consistent, in contrast to the *conventional local* approach investigated, e.g. in reference [23]. The transmission function approach is used as a benchmark, because it is not perturbative in the system-bath coupling. Furthermore, by resolving the energy dependence of heat transport, it indicates specific shortcomings in the other approaches. We include the local approach used in reference [23] to illustrate when and why the second law of thermodynamics may be violated.

In all five approaches, we take the so-called wide-band limit, assuming an energy-independent coupling between system and bath and neglecting any Lamb shift of the Hamiltonian. While this is the only assumption for the transmission approach, all master equation approaches further rely on the Born–Markov approximations. For the current scenario, these approximations are valid whenever

$$\kappa_\alpha \ll \Omega_\alpha, \tag{6}$$

where κ_α denotes the transition rate between system and reservoir $\alpha = c, h$. All master equation approaches are of the form

$$\partial_t \hat{\rho} = -i[\hat{H}_S, \hat{\rho}] + \mathcal{L}_c^j \hat{\rho} + \mathcal{L}_h^j \hat{\rho}, \tag{7}$$

with different dissipators $\mathcal{L}_\alpha^j$, where j labels the approach.

2.1. The transmission function

For non-interacting particles, the heat current can be written using a Landauer-like formula [42]. For bosons (with vanishing chemical potential) it takes on the form

$$J^t = \int_0^\infty \frac{d\omega}{2\pi} \mathcal{T}(\omega)\omega[n_B^h(\omega) - n_B^c(\omega)], \tag{8}$$

Figure 2. Steady state heat current for degenerate harmonic oscillators ($\Delta = 0$). (Grey) Transmission approach (J^{t}) which serves as a benchmark. The PERLind approach (J^{P}) agrees perfectly with the transmission approach for these figures. (Blue) Local approach (J^{l}). In steady state, this approach reduces to the conventional local approach (J^{cl}) for $\Delta = 0$. (Red) Global approach (J^{g}) which relies on the secular approximation. (a) As expected, the transmission approach interpolates between the local and global approaches as a function of the coupling strength g. In agreement with equation (15), the local approach may be justified even for $g > \kappa$. The insets illustrate the transmission function as a function of energy for two different values of g, where the local or the global approach is well justified. (b) The master equation approaches agree well with the transmission function approach for a wide range of temperatures. The inset (where $T_{\mathrm{c}} = 0$) illustrates the regime where both temperatures become small. We note that in this regime, the relative error associated to the master equation approaches may become large but the absolute error stays small. Parameters: $\kappa \equiv \kappa_{\mathrm{c}} = \kappa_{\mathrm{h}} = 0.02\,\bar{\Omega}$, $\Delta = 0$, $k_{\mathrm{B}}T_{\mathrm{h}} = \bar{\Omega}$, (a) $k_{\mathrm{B}}T_{\mathrm{c}} = 0.8\,\bar{\Omega}$, (b) $g = 5\kappa$, inset: $T_{\mathrm{c}} = 0$.

where we introduced the Bose–Einstein distribution

$$n_{\mathrm{B}}^{\alpha}(\omega) = \frac{1}{\mathrm{e}^{\frac{\omega}{k_{\mathrm{B}}T_{\alpha}}} - 1}, \tag{9}$$

and the transmission function $\mathcal{T}(\omega)$ can be obtained using non-equilibrium Green's functions [43, 44]. For the present system, it reads (see for instance reference [45] for the analogous case of Fermions)

$$\mathcal{T}(\omega) = \frac{g^2 \kappa_{\mathrm{c}} \kappa_{\mathrm{h}}}{\left| \left(\omega - \Omega_{\mathrm{h}} + \mathrm{i}\frac{\kappa_{\mathrm{h}}}{2} \right) \left(\omega - \Omega_{\mathrm{c}} + \mathrm{i}\frac{\kappa_{\mathrm{c}}}{2} \right) - g^2 \right|^2}. \tag{10}$$

The Landauer-like formula has an intuitive interpretation. At each energy ω, bosons traverse the system with the rate $\mathcal{T}(\omega)\mathrm{d}\omega$. The transmission function has two peaks located at Ω_+ and Ω_-. For small g and Δ, these peaks merge as illustrated in the insets of figure 2(b).

2.2. The conventional local approach
In this approach, the dissipators act locally on the two oscillators

$$\mathcal{L}_{\alpha}^{\mathrm{cl}} = \kappa_{\alpha} \left\{ n_{\mathrm{B}}^{\alpha}(\Omega_{\alpha}) \mathcal{D}[\hat{a}_{\alpha}^{\dagger}] + [n_{\mathrm{B}}^{\alpha}(\Omega_{\alpha}) + 1] \mathcal{D}[\hat{a}_{\alpha}] \right\}, \tag{11}$$

where cl stands for conventional local. Here we used the GKLS superoperators

$$\mathcal{D}[\hat{A}]\hat{\rho} = \hat{A}\hat{\rho}\hat{A}^{\dagger} - \frac{1}{2}\{\hat{A}^{\dagger}\hat{A}, \hat{\rho}\}, \tag{12}$$

with $\{\cdot, \cdot\}$ denoting the anti-commutator. The heat current in this approach is defined as

$$J^{\mathrm{cl}} = \mathrm{Tr}\left\{ \hat{H}_{\mathrm{S}} \mathcal{L}_{\mathrm{h}}^{\mathrm{cl}} \hat{\rho} \right\}. \tag{13}$$

In steady state, this reduces to

$$J^{\mathrm{cl}} = \frac{\kappa_{\mathrm{c}}\Omega_{\mathrm{h}} + \kappa_{\mathrm{h}}\Omega_{\mathrm{c}}}{(\kappa_{\mathrm{c}} + \kappa_{\mathrm{h}})^2} \frac{4g^2 \kappa_{\mathrm{c}}\kappa_{\mathrm{h}}[n_{\mathrm{B}}^{\mathrm{h}}(\Omega_{\mathrm{h}}) - n_{\mathrm{B}}^{\mathrm{c}}(\Omega_{\mathrm{c}})]}{4g^2 + \kappa_{\mathrm{c}}\kappa_{\mathrm{h}} + 16\Delta^2 \kappa_{\mathrm{c}}\kappa_{\mathrm{h}}/(\kappa_{\mathrm{c}} + \kappa_{\mathrm{h}})^2}. \tag{14}$$

It is important to note that there is a microscopic derivation that results in this local approach, which is valid for the current system as long as $n_{\mathrm{B}}^{\alpha}(\Omega_{\mathrm{h}}) \simeq n_{\mathrm{B}}^{\alpha}(\Omega_{\mathrm{c}})$ [13], which is the case for

$$g, \Delta \ll \bar{\Omega}. \tag{15}$$

When this inequality is satisfied, we may expect that the laws of thermodynamics hold, see figure 2. When this approximation is not justified, the second law of thermodynamics is not guaranteed as illustrated in figure 3. The reason for this is that the Bose–Einstein distributions are evaluated at Ω_{h} and Ω_{c} respectively in equation (14). This implies that the bosons change their energy when traversing the system. From the

Figure 3. Steady state heat current as a function of the detuning between the oscillator frequencies $\Delta = \Omega_h - \Omega_c$. (Grey) Transmission approach (J^t) which serves as a benchmark. The PERLind approach (J^p) agrees perfectly with the transmission approach for these figures. (Blue) Local approach (J^l). (Green) Conventional local approach (J^{cl}). (Red) Global approach (J^g). (a) For small coupling g, only a very small violation of the second law (negative heat current) is observed in the conventional local approach. (b) For larger g, the violation of the second law becomes larger. Interestingly, the local approach provides an accurate heat current, even though it is no longer microscopically justified for these parameters. Parameters: $\kappa \equiv \kappa_c = \kappa_h = 0.02\,\bar{\Omega}$, $k_B T_c = 0.8\,\bar{\Omega}$, $k_B T_h = \bar{\Omega}$, (a) $g = 0.02\,\bar{\Omega}$, (b) $g = 0.1\,\bar{\Omega}$.

Landauer-like formula (cf equation (8)), it is apparent that this cannot happen. We note that while equation (15) ensures $|n_B^\alpha(\Omega_h) - n_B^\alpha(\Omega_c)| \ll 1$, the relative error in the heat current can still be sizable when the occupation numbers (and thus the heat current) become small. This is the case because equation (15) does not ensure $|n_B^\alpha(\Omega_h) - n_B^\alpha(\Omega_c)| \ll n_B^\alpha(\Omega_\alpha)$.

2.3. Our local approach

Here we present a thermodynamically consistent local approach that follows from our general master equation introduced below in section 3, where we motivate this approach microscopically and show how it can be generalized to more complicated systems. As in the previous approach, the dissipators act locally in this approach

$$\mathcal{L}_\alpha^l = \kappa_\alpha \left\{ n_B^\alpha(\bar{\Omega})\mathcal{D}[\hat{a}_\alpha^\dagger] + [n_B^\alpha(\bar{\Omega}) + 1]\mathcal{D}[\hat{a}_\alpha] \right\}, \tag{16}$$

the only difference being that the Bose–Einstein distributions are now all evaluated at the frequency $\bar{\Omega}$. This approach has the same regime of validity as the previous local approach. Indeed, equation (15) implies

$$|n_B^\alpha(\bar{\Omega}) - n_B^\alpha(\Omega_\alpha)| \ll 1, \tag{17}$$

and we expect the dissipators in equations (11) and (16) to result in approximately the same dynamics as illustrated in figure 2. If equation (15) is not satisfied, the two local approaches may result in different results, see figure 3.

To obtain a thermodynamically consistent description, the approximation in equation (15) is exploited in the definition of the heat current which reads

$$J^l = \text{Tr}\left\{ \hat{H}_{TD}\mathcal{L}_h^l\hat{\rho} \right\}, \tag{18}$$

where we introduced a separate Hamiltonian for the thermodynamic bookkeeping (TD)

$$\hat{H}_{TD} = \bar{\Omega}(\hat{a}_c^\dagger\hat{a}_c + \hat{a}_h^\dagger\hat{a}_h). \tag{19}$$

Whenever equation (15) holds, this Hamiltonian provides the (approximately) correct energy flows. Consider the case where $\Delta = 0$. Then, $\hat{H}_{TD}$ is simply obtained by dropping the coupling between the oscillators. The thermodynamic bookkeeping thus neglects both the system-bath couplings, as well as the coupling between the oscillators. Of course, all these couplings are crucial for the dynamics, where they appear either in the Hamiltonian or in the dissipators. In section 3, we illustrate how such a thermodynamic Hamiltonian can be constructed in general, providing thermodynamic consistency of the corresponding master equation at the price of a slightly reduced energy resolution of thermodynamic quantities.

In steady state, the heat current reads

$$J^l = \frac{\bar{\Omega}}{\kappa_c + \kappa_h} \frac{4g^2\kappa_c\kappa_h[n_B^h(\bar{\Omega}) - n_B^c(\bar{\Omega})]}{4g^2 + \kappa_c\kappa_h + 16\Delta^2\kappa_c\kappa_h/(\kappa_c + \kappa_h)^2}. \tag{20}$$

We note that for $\Delta = 0$, we find $J^l = J^{cl}$ in the steady state. However, in the transient regime the two local approaches may result in different heat currents even for $\Delta = 0$. The difference between the two approaches

is in this case the energy associated to the coupling term (proportional to g), which is dropped in the local approach. We note that the heat current associated to this coupling term has been interpreted as a quantum contribution before [19].

Comparing the local master equation with the Landauer-like formula (cf equation (8)), one can see that transmission is approximated to happen at a single energy $\bar{\Omega}$. This is a good approximation when equation (15) holds. In this case, the transmission function is only non-zero around $\bar{\Omega}$ and the Bose–Einstein distributions may be assumed constant across all energies where transmission is non-zero. Interestingly, the local approach agrees well with the transmission approach for the present system, even when equation (15) is not satisfied, see figure 3(b). This is in stark contrast to the conventional local approach.

2.4. The global approach

In the global approach, the dissipators are introducing jumps between the eigenstates of the Hamiltonian

$$\mathcal{L}_\alpha^g = \sum_{\sigma=\pm} \kappa_\alpha^\sigma \left\{ n_B^\alpha(\Omega_\sigma)\mathcal{D}[\hat{a}_\sigma^\dagger] + [n_B^\alpha(\Omega_\sigma) + 1]\mathcal{D}[\hat{a}_\sigma] \right\}, \tag{21}$$

where the coupling strengths reflect the spatial distribution of the eigenstates

$$\kappa_h^+ = \kappa_h \cos^2(\theta/2), \quad \kappa_h^- = \kappa_h \sin^2(\theta/2), \quad \kappa_c^+ = \kappa_c \sin^2(\theta/2), \quad \kappa_c^- = \kappa_c \cos^2(\theta/2). \tag{22}$$

The heat current in the global approach reads

$$J^g = \mathrm{Tr}\left\{ \hat{H}_S \mathcal{L}_h^g \hat{\rho} \right\}, \tag{23}$$

which in steady state reduces to

$$J^g = \sum_{\sigma=\pm} \Omega_\sigma \frac{\kappa_c^\sigma \kappa_h^\sigma}{\kappa_c^\sigma + \kappa_h^\sigma} [n_B^h(\Omega_\sigma) - n_B^c(\Omega_\sigma)]. \tag{24}$$

This approach is thermodynamically consistent and we will always find heat flowing from hot to cold. As it relies on the secular approximation, it requires the condition

$$\kappa_c, \kappa_h \ll \sqrt{\Delta^2 + g^2}. \tag{25}$$

In the global master equation, the transmission is approximated to happen at the two energies $\Omega_\pm$. If equation (25) holds, the transmission function given in equation (10) consists of two narrow peaks located at $\Omega_\pm$, see the right inset in figure 2(b). Over the width of these peaks, the Bose–Einstein distributions can be assumed constant and the global master equation is valid. Note that if equation (25) does not hold, the peaks overlap and the secular approximation breaks down, see figure 2. We also note that equations (15) and (25) may both be valid. In this case, both the global as well as the local approach are expected to give accurate results.

2.5. The PERLind approach

In the PERLind approach, the dissipators read

$$\mathcal{L}_\alpha^p = \sum_{k=-1,1} \mathcal{D}[\hat{J}_{\alpha,k}], \tag{26}$$

with the jump operators

$$\hat{J}_{c,-1} = \sqrt{\kappa_c^+ [n_B^c(\Omega_+) + 1]}\hat{a}_+ + \sqrt{\kappa_c^- [n_B^c(\Omega_-) + 1]}\hat{a}_-,$$

$$\hat{J}_{c,1} = \sqrt{\kappa_c^+ n_B^c(\Omega_+)}\hat{a}_+^\dagger + \sqrt{\kappa_c^- n_B^c(\Omega_-)}\hat{a}_-^\dagger,$$

$$\hat{J}_{h,-1} = \sqrt{\kappa_h^+ [n_B^h(\Omega_+) + 1]}\hat{a}_+ - \sqrt{\kappa_h^- [n_B^h(\Omega_-) + 1]}\hat{a}_-, \tag{27}$$

$$\hat{J}_{h,1} = \sqrt{\kappa_h^+ n_B^h(\Omega_+)}\hat{a}_+^\dagger - \sqrt{\kappa_h^- n_B^h(\Omega_-)}\hat{a}_-^\dagger.$$

In this approach, the heat current is defined as

$$J^p = \mathrm{Tr}\left\{ \hat{H}_S \mathcal{L}_h^p \hat{\rho} \right\}. \tag{28}$$

For the present system, the heat current in the PERLind approach agrees perfectly with the result obtained from the transmission approach for all considered parameter values. This is expected as we consider scenarios where equation (6) is fulfilled and the Born–Markov approximations are justified. Clearly, the PERLind approach has strong advantages. However, it also has its disadvantages. First, the analytical expressions quickly become unwieldy, which is the case already for the simple system considered here. Second, the PERLind approach may violate the second law of thermodynamics [29]. When heat is defined by equation (28), a necessary and sufficient condition for the second law to hold is given by [46, 47]

$$\mathcal{L}_\alpha^\mathrm{p} e^{-\beta_\alpha \hat{H}_\mathrm{S}} = 0. \tag{29}$$

This condition is not fulfilled as shown in reference [30]. However, as long as the Born–Markov approximations are justified, any second law violations should become vanishingly small. It is an open question if a different definition for heat, that is consistent with the Born–Markov approximation, could salvage the second law.

2.6. Which approach to use?
As we have shown above, all approaches have their advantages and disadvantages. The PERLind approach provides the most accurate description, while the conventional local approach is the most simple, not requiring diagonalization of the Hamiltonian. Both approaches may however result in violations of the second law. The global and the local approach both respect the laws of thermodynamics. Furthermore, together they provide an accurate description for all parameter values as they are justified in complementary, but overlapping, parameter regimes (cf equations (6), (15) and (25), assuming the Born–Markov approximations are justified). In the following, we illustrate how these thermodynamically consistent approaches follow from a unified framework that can be extended to scenarios where neither a global nor a local description is justified.

3. A thermodynamically consistent master equation

We first revisit the general scenario under consideration and discuss the laws of thermodynamics. We then provide a detailed derivation and discuss how thermodynamic consistency is obtained by a consistent application of the approximations on the thermodynamic bookkeeping.

3.1. The general scenario
We consider the general scenario described by the Hamiltonian

$$\hat{H}_\mathrm{tot}(t) = \hat{H}_\mathrm{S}(t) + \sum_\alpha \left(\hat{H}_\alpha + \hat{V}_\alpha \right) = \hat{H}_\mathrm{S}(t) + \hat{H}_\mathrm{B} + \hat{V}, \tag{30}$$

where the first term describes the Hamiltonian of the system (which may be time-dependent) and the second and third term describe the thermal reservoirs (labeled by α) and their coupling to the system respectively. The system exchanges energy and particles with the reservoirs, such that energy changes can be divided into heat and work. The average heat that leaves bath α during the time interval $[0, t]$ is given by

$$\langle Q_\alpha \rangle = -\operatorname{Tr}\{(\hat{H}_\alpha - \mu_\alpha \hat{N}_\alpha)\hat{\rho}_\mathrm{tot}(t)\} + \operatorname{Tr}\{(\hat{H}_\alpha - \mu_\alpha \hat{N}_\alpha)\hat{\rho}_\mathrm{tot}(0)\}, \tag{31}$$

where $\hat{N}_\alpha$ denotes the particle number operator for reservoir α and μ_α its chemical potential. The average work provided by reservoir α is

$$\langle W_\alpha \rangle = -\mu_\alpha \left(\operatorname{Tr}\{\hat{N}_\alpha \hat{\rho}_\mathrm{tot}(t)\} - \operatorname{Tr}\{\hat{N}_\alpha \hat{\rho}_\mathrm{tot}(0)\} \right). \tag{32}$$

In addition, the time-dependence of the system Hamiltonian results in the external average power

$$P_\mathrm{ext}(t) = \operatorname{Tr}\{[\partial_t \hat{H}_\mathrm{S}(t)]\hat{\rho}_\mathrm{tot}(t)\}. \tag{33}$$

3.2. The laws of thermodynamics
Before deriving a Markovian description, we discuss the laws of thermodynamics as they hold for the general scenario.

3.2.1. The 0th law

For a large environment in thermal equilibrium (i.e. described by a single inverse temperature β and chemical potential μ) and a time-independent system Hamiltonian, the reduced state of the system tends to [48, 49]

$$\hat{\rho}_S = \mathrm{Tr}_B \left\{ e^{-\beta(\hat{H}_{tot} - \mu \hat{N}_{tot})} / Z \right\}, \quad Z = \mathrm{Tr} \left\{ e^{-\beta(\hat{H}_{tot} - \mu \hat{N}_{tot})} \right\}, \tag{34}$$

where Tr_B denotes the trace over the reservoir degrees of freedom. In the weak system-bath coupling limit, equation (34) reduces to the Gibbs state

$$\hat{\rho}_S = \frac{e^{-\beta(\hat{H}_S - \mu \hat{N}_S)}}{\mathrm{Tr} \left\{ e^{-\beta(\hat{H}_S - \mu \hat{N}_S)} \right\}}. \tag{35}$$

3.2.2. The 1st law

For future reference, we first introduce the heat current and power provided by bath α as

$$J_\alpha(t) = \partial_t \langle Q_\alpha \rangle, \qquad P_\alpha(t) = \partial_t \langle W_\alpha \rangle. \tag{36}$$

The first law of thermodynamics is then given by

$$\partial_t U(t) = P_{ext}(t) + \sum_\alpha [J_\alpha(t) + P_\alpha(t)], \quad U = \mathrm{Tr}\{[\hat{H}_S(t) + \hat{V}]\hat{\rho}_{tot}(t)\}. \tag{37}$$

In the weak system-bath coupling limit, the coupling energy can be neglected and $U = \mathrm{Tr}\{\hat{H}_S(t)\hat{\rho}_{tot}(t)\}$ reduces to the usual internal energy of the system.

3.2.3. The 2nd law

To express the second law of thermodynamics, we impose the initial condition

$$\hat{\rho}_{tot}(0) = \hat{\rho}_S(0) \bigotimes_\alpha \hat{\tau}_\alpha, \quad \hat{\tau}_\alpha = \frac{e^{-\beta(\hat{H}_\alpha - \mu \hat{N}_\alpha)}}{\mathrm{Tr}\left\{ e^{-\beta_\alpha(\hat{H}_\alpha - \mu_\alpha \hat{N}_\alpha)} \right\}}, \tag{38}$$

i.e. all reservoirs are in local thermal equilibrium and uncorrelated with the system and the other reservoirs. With this initial condition, the second law of thermodynamics can be written as [50]

$$\Sigma(t) \equiv \Delta S(t) - \sum_\alpha \frac{\langle Q_\alpha \rangle}{T_\alpha} = S\left[\hat{\rho}_{tot}(t) \| \hat{\rho}_S(t) \bigotimes_\alpha \hat{\tau}_\alpha \right] \geqslant 0, \tag{39}$$

where $\hat{\rho}_S = \mathrm{Tr}_B\{\hat{\rho}_{tot}(t)\}$ denotes the reduced state of the system, $S[\hat{\rho}_1 \| \hat{\rho}_2] = \mathrm{Tr}\{\hat{\rho}_1(\ln \hat{\rho}_1 - \ln \hat{\rho}_2)\}$ is the quantum relative entropy (which is by definition positive for positive definite density matrices $\hat{\rho}_1, \hat{\rho}_2$ with unity trace), and ΔS denotes the change in the system's von Neumann entropy

$$\Delta S(t) = -k_B \, \mathrm{Tr}\{\hat{\rho}_S(t) \ln \hat{\rho}_S(t)\} + k_B \, \mathrm{Tr}\{\hat{\rho}_S(0) \ln \hat{\rho}_S(0)\}. \tag{40}$$

Equation (39) has an intuitive interpretation: the entropy production Σ denotes the information that is lost when describing system and reservoirs by the state $\hat{\rho}_S(t)\bigotimes_\alpha \hat{\tau}_\alpha$. In this description, correlations between the system and the reservoirs, as well as any displacement from equilibrium of the reservoirs are neglected [51].

While equation (39) is always non-negative, the same is not necessarily true for the entropy production rate

$$\dot{\Sigma}(t) \equiv \partial_t \Delta S(t) - \sum_\alpha \frac{J_\alpha(t)}{T_\alpha}. \tag{41}$$

A negative entropy production rate can be understood as *information backflow* and is a hallmark of non-Markovian behavior [52]. For systems amenable to a Markovian description, we expect $\dot{\Sigma} \geqslant 0$, as the initial condition in equation (38) can be translated in time without altering the dynamics.

3.3. Distribution for heat and work exchanged with the reservoirs

Throughout this work, we are mainly interested in average thermodynamic quantities. In order to obtain a Markovian description of these, it is nevertheless instructive to start with the full probability distribution for the heat and work exchanged with the reservoirs. With the initial condition given in equation (38), this distribution can be written as

$$P(\boldsymbol{Q}, \boldsymbol{W}) = \sum_{\boldsymbol{E}, \boldsymbol{E'}, \boldsymbol{N}, \boldsymbol{N'}} P_t(\boldsymbol{E'}, \boldsymbol{N'}|\boldsymbol{E}, \boldsymbol{N}) P_0(\boldsymbol{E}, \boldsymbol{N})$$

$$\times \prod_{\alpha} \delta(W_\alpha - \mu_\alpha N'_\alpha + \mu_\alpha N_\alpha) \delta(Q_\alpha + W_\alpha - E'_\alpha + E_\alpha), \tag{42}$$

where we grouped Q_α, W_α, E_α, and N_α into vectors $\boldsymbol{Q}$, $\boldsymbol{W}$, $\boldsymbol{E}$, and $\boldsymbol{N}$ and similarly for E'_α and N'_α. The joint probability for each bath α having energy E_α and particle number N_α at time $t = 0$ is given by

$$P_0(\boldsymbol{E}, \boldsymbol{N}) = \prod_\alpha \frac{e^{-\beta_\alpha(E_\alpha - \mu_\alpha N_\alpha)}}{\text{Tr}\left\{e^{-\beta_\alpha(\hat{H}_\alpha - \mu_\alpha \hat{N}_\alpha)}\right\}}. \tag{43}$$

The conditional probability that the reservoirs have energies E'_α and particle number N'_α at time t, given that their energies and particle numbers where E_α and N_α initially reads

$$P_t(\boldsymbol{E'}, \boldsymbol{N'}|\boldsymbol{E}, \boldsymbol{N}) = \text{Tr}\{\hat{M}\hat{\rho}_\text{S}(0)\hat{M}^\dagger\}, \quad \hat{M} = \text{Tr}_\text{B}\{|\boldsymbol{E}, \boldsymbol{N}\rangle\langle \boldsymbol{E'}, \boldsymbol{N'}|\hat{U}(t)\}, \tag{44}$$

where $\hat{H}_\alpha|\boldsymbol{E}, \boldsymbol{N}\rangle = E_\alpha|\boldsymbol{E}, \boldsymbol{N}\rangle$, $\hat{N}_\alpha|\boldsymbol{E}, \boldsymbol{N}\rangle = N_\alpha|\boldsymbol{E}, \boldsymbol{N}\rangle$, and we introduced the time-evolution operator

$$\hat{U}(t) = \mathcal{T} e^{-i\int_0^t dt' \hat{H}_\text{tot}(t')}, \tag{45}$$

with $\mathcal{T}$ denoting the time-ordering operator. We note that the probability distribution given in (42) can in principle be measured by applying projective measurements on the reservoirs at the initial and final time. Importantly, while such measurements may not be experimentally feasible, they do not influence the dynamics of the system due to the chosen initial condition.

The moment generating function is provided by the Fourier transform of the probability distribution in (42)

$$\Lambda(\boldsymbol{\lambda}, \boldsymbol{\chi}) \equiv \int d\boldsymbol{Q}\, d\boldsymbol{W} P(\boldsymbol{Q}, \boldsymbol{W}) e^{-i\boldsymbol{\lambda}\cdot\boldsymbol{Q} - i\boldsymbol{\chi}\cdot\boldsymbol{W}} = \text{Tr}\left\{\hat{\rho}_\text{tot}(\boldsymbol{\lambda}, \boldsymbol{\chi}; t)\right\}, \tag{46}$$

where we introduced

$$\hat{\rho}_\text{tot}(\boldsymbol{\lambda}, \boldsymbol{\chi}; t) = \hat{U}(\boldsymbol{\lambda}, \boldsymbol{\chi}; t)\hat{\rho}_\text{tot}(0)\hat{U}^\dagger(-\boldsymbol{\lambda}, -\boldsymbol{\chi}; t) \tag{47}$$

with the modified time-evolution operator

$$\hat{U}(\boldsymbol{\lambda}, \boldsymbol{\chi}; t) = e^{-\frac{i}{2}\sum_\alpha [\lambda_\alpha(\hat{H}_\alpha - \mu_\alpha \hat{N}_\alpha) + \chi_\alpha \mu_\alpha \hat{N}_\alpha]} \hat{U}(t) e^{\frac{i}{2}\sum_\alpha [\lambda_\alpha(\hat{H}_\alpha - \mu_\alpha \hat{N}_\alpha) + \chi_\alpha \mu_\alpha \hat{N}_\alpha]}. \tag{48}$$

The quantities λ_α and χ_α are known as counting fields and allow us to keep track of work and heat exchanged with the reservoirs (for the use of counting fields in master equations, see references [4, 53]). From the moment generating function, we recover the average values for heat and work given in section 3.1 as

$$\langle Q_\alpha \rangle = i\partial_{\lambda_\alpha} \Lambda(\boldsymbol{\lambda}, 0)|_{\boldsymbol{\lambda}=0}, \qquad \langle W_\alpha \rangle = i\partial_{\chi_\alpha} \Lambda(0, \boldsymbol{\chi})|_{\boldsymbol{\chi}=0}. \tag{49}$$

We note that we do not include the external power in the probability distribution for heat and work as this goes beyond the scope of this paper. Indeed, fluctuations of the external power may not necessarily be described by a positive probability distribution without introducing a measurement scheme that potentially alters the dynamics of the system [54–56].

3.4. Born–Markov approximations
We are now in a position to derive a Markovian master equation, keeping track of the thermodynamic bookkeeping associated to the heat and work exchanged with the bath. Together with a secular approximation, resulting in a *global* master equation, such a procedure has been applied before [57–59] (for a similar approach based on path-integrals, see [60]). Here we will make an approximation that is different from the secular approximation, allowing for treating (near) degeneracies while still ensuring thermodynamic consistency. We follow standard procedure [1, 4] and write the system-bath coupling as

$$\hat{V} = \sum_{\alpha, k} \hat{S}_{\alpha, k} \hat{B}_{\alpha, k}, \tag{50}$$

where the operators $\hat{S}_{\alpha, k}$ ($\hat{B}_{\alpha, k}$) act only on the system (reservoir). We note that we do not assume that these operators are Hermitian. To determine the jump operators that will enter the Markovian master equation, we need the Fourier coefficients of the operators $\hat{S}_{\alpha, k}$ in the interaction picture, i.e.

$$\hat{U}_\text{S}^\dagger(t)\hat{S}_{\alpha, k}\hat{U}_\text{S}(t) = \sum_j e^{-i\omega_j t}\hat{S}_{\alpha, k; j}, \quad \hat{U}_\text{S}(t) = \mathcal{T} e^{-i\int_0^t dt' \hat{H}_\text{S}(t')}. \tag{51}$$

For a time-independent Hamiltonian, the frequencies ω_j denote the energy gaps in the Hamiltonian and the operators $\hat{S}_{\alpha,k;j}$ are ladder operators that induce transitions between the corresponding states. For a periodic Hamiltonian with period $t_\mathrm{p} = 2\pi/\varpi$, the $\hat{S}_{\alpha,k;j}$ are ladder operators of an averaged Hamiltonian defined by

$$\hat{U}_\mathrm{S}(t_\mathrm{p}) = \mathrm{e}^{-\mathrm{i}\hat{H}_\mathrm{av} t_\mathrm{p}}. \tag{52}$$

The frequencies then fulfill $\omega_j = \nu_j + l_j\varpi$, where ν_j denotes an energy gap of $\hat{H}_\mathrm{av}$ and l_j denotes an integer, corresponding to the exchange of photons with the driving field [57, 61, 62].

Standard application of Born–Markov approximations then results in the Redfield equation including counting fields (in the interaction picture)

$$\partial_t\hat{\rho}_\mathrm{S}(t) = -\sum_{\alpha,k,k',j,j'} \mathrm{e}^{\mathrm{i}(\omega_j - \omega_{j'})t} \int_0^\infty \mathrm{d}s\, \mathcal{I}(s,t),$$

$$\mathcal{I}(s,t) = \mathrm{e}^{\mathrm{i}\omega_{j'}s} C_{k,k'}^\alpha(s)\hat{S}_{\alpha,k;j}^\dagger \hat{S}_{\alpha,k';j'}\hat{\rho}_\mathrm{S}(t) + \mathrm{e}^{-\mathrm{i}\omega_j s} C_{k,k'}^\alpha(-s)\hat{\rho}_\mathrm{S}(t)\hat{S}_{\alpha,k;j}^\dagger \hat{S}_{\alpha,k';j'}$$

$$- \mathrm{e}^{\mathrm{i}\mu_\alpha n_{\alpha,k}(\lambda_\alpha - \chi_\alpha)}\left[\mathrm{e}^{\mathrm{i}\omega_{j'}s} C_{k,k'}^\alpha(s + \lambda_\alpha) + \mathrm{e}^{-\mathrm{i}\omega_j s} C_{k,k'}^\alpha(-s + \lambda_\alpha)\right]\hat{S}_{\alpha,k';j'}\hat{\rho}_\mathrm{S}(t)\hat{S}_{\alpha,k;j}^\dagger, \tag{53}$$

where we suppressed the counting field dependence of the density matrix for ease of notation. We note that the term *Redfield equation* sometimes refers to the non-Markovian equation that is obtained before taking the time-integration to infinity [1] while we include this limit here. Here we used global particle conservation, which ensures

$$[\hat{S}_{\alpha,k;j}, \hat{N}_\mathrm{S}] = n_{\alpha,k}\hat{S}_{\alpha,k;j}, \qquad [\hat{S}_{\alpha,k';j'}, \hat{N}_\mathrm{S}] = n_{\alpha,k}\hat{S}_{\alpha,k';j'}, \tag{54}$$

for all pairs k and k' that appear together in equation (53), i.e. $\hat{S}_{\alpha,k;j}$ and $\hat{S}_{\alpha,k';j'}$ change the particle number by the same amount, such that no superpositions of particle numbers are created. We further introduced the bath correlation functions

$$C_{k,k'}^\alpha(s) = \mathrm{Tr}\left\{\mathrm{e}^{\mathrm{i}s\hat{H}_\alpha}\hat{B}_{\alpha,k}^\dagger \mathrm{e}^{-\mathrm{i}s\hat{H}_\alpha}\hat{B}_{\alpha,k'}\hat{\tau}_\alpha\right\}. \tag{55}$$

These correlation functions define a bath correlation time τ_B by their characteristic decay time. The Markov approximation is generally justified when the bath correlation time is much shorter than the characteristic time-scale over which $\hat{\rho}_\mathrm{S}$ changes in the interaction picture, τ_S. The time τ_S describes the relaxation time of the system and is determined by the inverse of the system-bath coupling. Note however that the counting fields λ_α enter the argument of the bath correlation times. For the counting-field dependent density matrix, the Markov approximation is only justified if $C_{k,k'}^\alpha(\pm\tau + \lambda_\alpha) \simeq 0$ for $\tau \gtrsim \tau_\mathrm{S}$. This implies the regime of validity

$$\tau_\mathrm{B} \ll \tau_\mathrm{S}, \quad |\lambda_\alpha| \ll \tau_\mathrm{S}. \tag{56}$$

The last inequality has a very important consequence. It implies that only the low frequency components of the heat distribution are to be trusted. Due to the uncertainty principle between Fourier conjugate variables [63], this implies that energy-differences in heat of the order of $1/\tau_\mathrm{S}$ cannot be resolved. Thus, whenever a Markovian description is employed, the heat exchanged with the reservoirs suffers from a limited energy-resolution. With this in mind, it is no surprise that Markovian descriptions may result in thermodynamic inconsistencies. There is however a straightforward solution to the problem: as our resolution of heat is finite, we may change the definition of heat such that it fulfills the laws of thermodynamics while remaining the same within our limited resolution.

3.5. Frequency grouping for positivity

It is well known that the Redfield equation does not preserve positivity of the density matrix and can thus result in negative probabilities. Multiple schemes have been put forward to achieve positivity. Here we introduce a novel scheme that has the same regime of validity as the Born–Markov assumptions and thus goes beyond the regime of validity of the secular approximation. As we show in the next subsection, our approach allows for a thermodynamically consistent formulation.

Equation (56) ensures that for any two transition frequencies we either have $|\omega_j - \omega_{j'}| \ll 1/\tau_\mathrm{B}$ or $|\omega_j - \omega_{j'}| \gg 1/\tau_\mathrm{S}$. Indeed, both of these conditions may be fulfilled simultaneously as $\tau_\mathrm{B} \ll \tau_\mathrm{S}$. We may thus group the transition frequencies into sets x_q, such that the first (second) inequality holds if the transition frequencies are in the same (different) set, that is

$$|\omega_j - \omega_{j'}| \ll 1/\tau_\mathrm{B} \quad \text{for } \omega_j \in x_q,\ \omega_{j'} \in x_{q'} \text{ with } q = q',$$

$$|\omega_j - \omega_{j'}| \gg 1/\tau_\mathrm{S} \quad \text{for } \omega_j \in x_q,\ \omega_{j'} \in x_{q'} \text{ with } q \neq q'. \tag{57}$$

It is important to note that this procedure may not always work, for instance if the ω_j form a continuum. However, in small quantum systems, where the number of transition frequencies is finite, this procedure is expected to work. It is particularly well suited for thermal machines that consist of weakly coupled sub-units. These naturally exhibit sets of near-degenerate transition frequencies (see the examples below).

In the spirit of the secular approximation, we then drop terms in equation (53) where ω_j and $\omega_{j'}$ belong to different sets. This is justified as the corresponding terms exhibit fast oscillations that average to zero. For transition frequencies in the same set x_q, we follow the spirit of the Markov approximation and replace

$$e^{i\omega_j s}, e^{i\omega_{j'} s} \to e^{i\omega_q s}, \qquad |\omega_q - \omega_j| \ll 1/\tau_B \quad \forall \; \omega_j \in x_q, \tag{58}$$

within $\mathcal{I}(s)$ in equation (53), while keeping the frequency differences in the prefactor $e^{i(\omega_j - \omega_{j'})t}$ governing the coherent dynamics of the system. For each set, we thus choose a *set frequency* ω_q. All transition frequencies ω_j in the set x_q are then replaced by the set frequency, because they are virtually indistinguishable over the time-scale over which the integrand in equation (53) is finite.

This approximation results in the Lindblad master equation

$$\partial_t \hat{\rho}_S(\boldsymbol{\lambda}, \boldsymbol{\chi}; t) = -i[\hat{H}_{LS}, \hat{\rho}_S(\boldsymbol{\lambda}, \boldsymbol{\chi}; t)] + \sum_\alpha \tilde{\mathcal{L}}_\alpha^{\chi_\alpha, \lambda_\alpha} \hat{\rho}_S(\boldsymbol{\lambda}, \boldsymbol{\chi}; t), \tag{59}$$

with

$$\tilde{\mathcal{L}}_\alpha^{\chi_\alpha, \lambda_\alpha} \hat{\rho} = \sum_{k;q} \Gamma_k^\alpha(\omega_q) \left[e^{-i\lambda_\alpha \omega_q - i(\chi_\alpha - \lambda_\alpha)\mu_\alpha n_{\alpha,k}} \hat{S}_{\alpha,k;q}(t) \hat{\rho} \hat{S}_{\alpha,k;q}^\dagger(t) - \frac{1}{2} \left\{ \hat{S}_{\alpha,k;q}^\dagger(t) \hat{S}_{\alpha,k;q}(t), \hat{\rho} \right\} \right], \tag{60}$$

where the tilde denotes the interaction picture and we introduced the jump operators

$$\hat{S}_{\alpha,k;q}(t) = \sum_{\{j | \omega_j \in x_q\}} e^{-i\omega_j t} \hat{S}_{\alpha,k;j}, \tag{61}$$

and the Lamb-shift Hamiltonian

$$\hat{H}_{LS} = \sum_{\alpha,k;q} \Delta_k^\alpha(\omega_q) \hat{S}_{\alpha,k;q}^\dagger(t) \hat{S}_{\alpha,k;q}(t), \tag{62}$$

as well as the quantities

$$\Gamma_k^\alpha(\omega) = \int_{-\infty}^\infty ds \, e^{i\omega s} C_{k,k}^\alpha(s) \qquad \Delta_k^\alpha(\omega) = -\frac{i}{2} \int_{-\infty}^\infty ds \, e^{i\omega s} \, \text{sign}(s) C_{k,k}^\alpha(s). \tag{63}$$

For simplicity, we assumed $C_{k,k'}^\alpha \propto \delta_{k,k'}$ to derive equation (59). We note that relaxing this assumption is straightforward.

In the absence of counting fields, we may use the Kubo–Martin–Schwinger condition [1] (which is slightly complicated by our definition of the bath-correlation functions) to write the master equation as

$$\partial_t \hat{\rho}_S = -i[\hat{H}_{LS}(t), \hat{\rho}_S] + \sum_\alpha \tilde{\mathcal{L}}_\alpha \hat{\rho}_S, \tag{64}$$

with

$$\tilde{\mathcal{L}}_\alpha = \sum_{\{q | \omega_q > 0\}} \sum_k \Gamma_k^\alpha(\omega_q) \left\{ \mathcal{D}[\hat{S}_{\alpha,k;q}(t)] + e^{-\beta_\alpha(\omega_q - \mu_\alpha n_{\alpha,k})} \mathcal{D}[\hat{S}_{\alpha,k;q}^\dagger(t)] \right\}. \tag{65}$$

For a time-independent Hamiltonian, the master equation in the Schrödinger picture is given by

$$\partial_t \hat{\rho}_S = -i[\hat{H}_S + \hat{H}_{LS}, \hat{\rho}_S] + \sum_\alpha \mathcal{L}_\alpha \hat{\rho}_S, \tag{66}$$

with

$$\mathcal{L}_\alpha = \sum_{\{q | \omega_q > 0\}} \sum_k \Gamma_k^\alpha(\omega_q) \left\{ \mathcal{D}[\hat{S}_{\alpha,k;q}] + e^{-\beta_\alpha(\omega_q - \mu_\alpha n_{\alpha,k})} \mathcal{D}[\hat{S}_{\alpha,k;q}^\dagger] \right\}. \tag{67}$$

where $\hat{S}_{\alpha,k;q} \equiv \hat{S}_{\alpha,k;q}(0)$ and $\hat{H}_{LS} \equiv \hat{H}_{LS}(0)$. For time-dependent Hamiltonians, one has to be more careful because in general $\hat{S}_{\alpha,k;q}(t) \neq \hat{U}_S^\dagger(t) \hat{S}_{\alpha,k;q} \hat{U}_S(t)$, see also appendix A.

There are two simple limits for the master equation in equation (66). If all pairs of transition frequencies fulfill $|\omega_j - \omega_{j'}| \gg 1/\tau_S$, then each transition frequency may be associated to a separate set x_j. We then recover the secular approximation where $\mathcal{D}[\hat{S}_{\alpha,k;q}(t)] = \mathcal{D}[\hat{S}_{\alpha,k;j}]$ (the time-dependence of the jump

operators drops out in the interaction picture). If all pairs of transition frequencies fulfill $|\omega_j - \omega_{j'}| \ll 1/\tau_B$, then all transition frequencies may be grouped into a single set x_0 such that $\hat{S}_{\alpha,k;q}(t) = \hat{U}_S^\dagger(t)\hat{S}_{\alpha,k}\hat{U}_S(t)$ (the time-dependence of the jump operators drops out upon returning to the Schrödinger picture). We then recover a local master equation, which has the appeal that the Hamiltonian does not need to be diagonalized in order to identify the jump operators. This local approach differs from the conventional local approach as only a single frequency enters the bath distribution function.

Importantly, the counting fields λ_α have an influence on the regime of validity of equation (59), just as for the Markov approximation. Indeed, for the approximation to be valid, $|\omega_q - \omega_j|$ does not only have to be much smaller than $1/\tau_B$ but also has to be much smaller than $1/|\lambda_\alpha|$ (in complete analogy to equation (56)). Just like the Markov approximation, this frequency-grouping thus limits the energy-resolution for heat exchanged with the reservoirs. As a consequence, energy changes of the order of $|\omega_j - \omega_{j'}|$, where both frequencies are within the same set, can no longer be resolved. This finite resolution in energy may result in the false conclusion that particles change their energy when traversing the system. In the conventional local approach, this results in thermodynamic inconsistencies when using standard definitions for heat, see section 2.

We note that dropping terms that involve frequencies from different sets is reminiscent of the partial secular approximation developed in references [15, 34, 35, 64, 65]. Here, as well as in reference [41], an additional coarse-graining in energy (replacing frequencies with set-frequencies) results in a master equation in GKLS form.

3.6. Two Hamiltonians for thermodynamic consistency

We now turn to the question of how to utilize the finite energy-resolution to ensure thermodynamic consistency. To do this, we introduce a second Hamiltonian, $\hat{H}_{TD}$, that provides the correct thermodynamic bookkeeping under the approximations that resulted in our master equation. For simplicity, we consider here a time-independent system Hamiltonian. The time-dependent case is slightly more complicated and treated in appendix A. Due to the frequency grouping outlined in the last subsection, all frequencies in the set x_q are effectively replaced by the frequency ω_q from the point of view of the reservoirs. To ensure a consistent thermodynamic bookkeeping, the Hamiltonian $\hat{H}_{TD}$ needs to fulfill

$$[\hat{S}_{\alpha,k;j}, \hat{H}_{TD}] = \omega_q \hat{S}_{\alpha,k;j}, \tag{68}$$

for all frequencies $\omega_j \in x_q$. To fulfill this, the thermodynamic Hamiltonian can be obtained from $\hat{H}_S$ by changing its eigenvalues such that all frequencies $\omega_j \to \omega_q$ for $\omega_j \in x_q$. Such a rescaling is expected to always be possible if the frequency grouping is possible as discussed above.

With the thermodynamic Hamiltonian at hand, we define the internal energy of the system as

$$U = \text{Tr}\{\hat{H}_{TD}\hat{\rho}\}. \tag{69}$$

Furthermore, from equations (59), (36), and (49) we find that the heat current and power provided by bath α can be cast into

$$J_\alpha = \text{Tr}\{(\hat{H}_{TD} - \mu_\alpha \hat{N}_S)\mathcal{L}_\alpha \hat{\rho}_S\}, \qquad P_\alpha = \mu_\alpha \, \text{Tr}\{\hat{N}_S \mathcal{L}_\alpha \hat{\rho}_S\}, \tag{70}$$

where $\mathcal{L}_\alpha$ is defined in equation (67). We note that while $\hat{H}_{TD}$ determines the thermodynamic bookkeeping, it is still $\hat{H}_S$ that determines the kinetics, i.e. enters the master equation in equation (59). For future reference, we also introduce the total power produced by the system as

$$P_S(t) = -\sum_\alpha P_\alpha(t) - P_{ext}(t). \tag{71}$$

This will be the quantity of interest when we consider heat engines.

3.6.1. The 0th law

Using equation (68), it is straightforward to show that

$$\mathcal{L}_\alpha e^{-\beta_\alpha(\hat{H}_{TD} - \mu_\alpha \hat{N}_S)} = 0. \tag{72}$$

as well as $[\hat{H}_{TD}, \hat{H}_{LS}] = 0$. Furthermore, as $\hat{H}_{TD}$ is obtained by changing only the eigenvalues of $\hat{H}_S$, these two Hamiltonians also commute. When all reservoirs have the same inverse temperature β and chemical potential μ, it then follows that the Gibbs state with respect to the thermodynamic Hamiltonian,

$$\hat{\rho}_G(\beta, \mu) = \frac{e^{-\beta(\hat{H}_{TD} - \mu \hat{N}_S)}}{\text{Tr}\{e^{-\beta(\hat{H}_{TD} - \mu \hat{N}_S)}\}}, \tag{73}$$

is the steady state of equation (66). Compared to equation (35), this state neglects the system-bath coupling, as well as the differences between $\hat{H}_S$ and $\hat{H}_{TD}$. This is consistent with our approximations, which imply that these differences cannot be resolved within our Markovian treatment.

3.6.2. The first law
Using $[\hat{H}_{TD}, \hat{H}_S + \hat{H}_{LS}] = 0$, the first law of thermodynamics follows directly from equations (69) and (70) and reads

$$\partial_t U = \sum_\alpha (P_\alpha + J_\alpha). \tag{74}$$

3.6.3. The second law
The entropy production rate can be written as

$$\dot{\Sigma}/k_B = -\partial_t \, \mathrm{Tr}\{\hat{\rho}_S \ln \hat{\rho}_S\} - \sum_\alpha \beta_\alpha J_\alpha = -\sum_\alpha \mathrm{Tr}\{(\mathcal{L}_\alpha \hat{\rho}_S)[\ln \hat{\rho}_S - \ln \hat{\rho}_G(\beta_\alpha, \mu_\alpha)]\} \geqslant 0. \tag{75}$$

Here we used equations (66), (70), and the last inequality is known as Spohns inequality [46, 66] and relies on $\hat{\rho}_G(\beta_\alpha, \mu_\alpha)$ being a fixed point of $\mathcal{L}_\alpha$, cf equation (72).

The master equation in equation (66), together with the thermodynamic bookkeeping introduced in equations (69) and (70), thus provide a thermodynamically consistent description. We stress that the only assumption that went into equation (66) is the one that justifies the standard Born–Markov approximations, i.e. $\tau_B \ll \tau_S$. However, when considering the full probability distribution for heat and work exchanged with the reservoirs, cf (59), then we further have restrictions on the counting fields λ_α which are the Fourier transform variables of heat. These restrictions imply that we lose energy-resolution on the scale of $1/\tau_S$ as well as $|\omega_j - \omega_j'|$ for pairs of frequencies that are close to each other (and grouped into one set). Thermodynamic consistency is obtained by using an appropriate definition of heat that is consistent with our limited energy-resolution (i.e. we may freely add terms of order $|\omega_j - \omega_j'|$ to heat, as our results are not to be trusted to this order in the first place).

4. Fermionic heat engine

4.1. System
In this section, we illustrate the derivation of our master equation for a simple but non-trivial example of non-interacting electrons. Here, as well as for all time-independent examples, we provide all equations in the Schrödinger picture. The system under consideration is sketched in figure 4 and consists of two coupled single-level quantum dots

$$\hat{H}_S = \Omega_L \hat{d}_L^\dagger \hat{d}_L + \Omega_R \hat{d}_R^\dagger \hat{d}_R + g(\hat{d}_L^\dagger \hat{d}_R + \hat{d}_R^\dagger \hat{d}_L), \tag{76}$$

with the standard anti-commutation relations

$$\{\hat{d}_\alpha, \hat{d}_\beta^\dagger\} = \delta_{\alpha,\beta}, \qquad \{\hat{d}_\alpha, \hat{d}_\beta\} = 0. \tag{77}$$

In equation (76), Ω_α denote the on-site energies and g the coupling strength. We note that this system is a fermionic version of the system considered in section 2 and thus shares many of its properties. Due to the finite chemical potential of the reservoirs, it can however feature as a heat engine, leveraging a heat current to drive a particle current against a chemical potential bias. The reservoirs and their coupling to the system are described by

$$\hat{H}_\alpha = \sum_l \varepsilon_{\alpha,l} \hat{c}_{\alpha,l}^\dagger \hat{c}_{\alpha,l}, \qquad \hat{V}_\alpha = \sum_l t_{\alpha,l}(\hat{d}_\alpha^\dagger \hat{c}_{\alpha,l} + \hat{c}_{\alpha,l}^\dagger \hat{d}_\alpha), \tag{78}$$

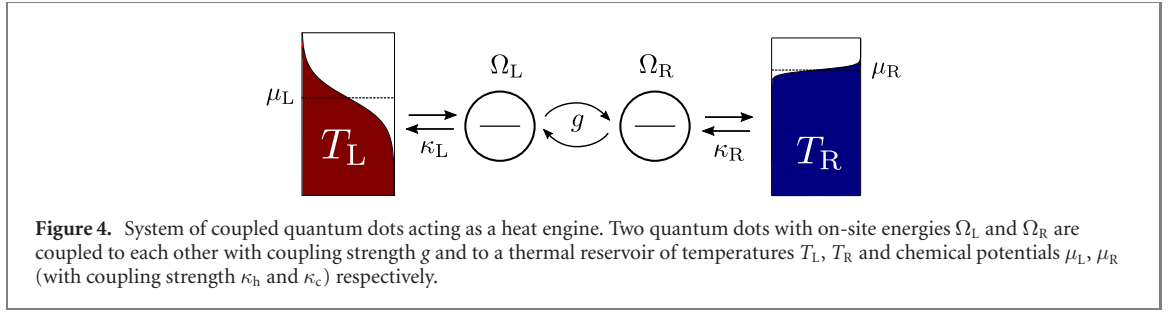with $\alpha = L, R$. From equations (50) and (78), we identify the following system and bath operators

$$\hat{S}_{\alpha,1} = \hat{d}_\alpha^\dagger, \qquad \hat{S}_{\alpha,-1} = \hat{d}_\alpha, \tag{79}$$

and

$$\hat{B}_{\alpha,1} = \sum_l t_{\alpha,l} \hat{c}_{\alpha,l}, \qquad \hat{B}_{\alpha,-1} = \sum_l t_{\alpha,l} \hat{c}_{\alpha,l}^\dagger. \tag{80}$$

To derive the master equation and judge its validity, the bath correlation functions need to be inspected. We defer this discussion to appendix B.1, and simply state the conclusion that the Born Markov approximations are valid whenever

$$\kappa_\alpha \ll \max\{k_B T_\beta, |\omega_j - \mu_\beta|\}, \tag{81}$$

Figure 4. System of coupled quantum dots acting as a heat engine. Two quantum dots with on-site energies Ω_L and Ω_R are coupled to each other with coupling strength g and to a thermal reservoir of temperatures T_L, T_R and chemical potentials μ_L, μ_R (with coupling strength κ_h and κ_c) respectively.

where the inequality should hold for all choices of α, β, and j and we assumed an energy-independent bath spectral density. Physically, equation (81) ensures that the rates

$$\Gamma_1^\alpha(-\omega) = \kappa_\alpha n_F^\alpha(\omega), \qquad \Gamma_{-1}^\alpha(\omega) = \kappa_\alpha[1 - n_F^\alpha(\omega)], \tag{82}$$

with the Fermi–Dirac distribution

$$n_F^\alpha(\omega) = \frac{1}{e^{\frac{\omega - \mu_\alpha}{k_B T_\alpha}} + 1}, \tag{83}$$

is flat over the energy scale κ_α. At high temperatures, this is ensured because the Fermi–Dirac distribution becomes flat. For large $|\omega_j - \mu_\beta|$, the eigenenergies of the double quantum dot lie far away from the chemical potential, where the Fermi–Dirac distribution is flat and takes on the value zero or one.

To identify the transition frequencies and the jump operators, we require the Fourier coefficients of the system operators given in equation (79)

$$e^{i\hat{H}_S t}\hat{d}_R e^{-i\hat{H}_S t} = e^{-i\Omega_- t}\cos(\theta/2)\hat{d}_- + e^{-i\Omega_+ t}\sin(\theta/2)\hat{d}_+,$$
$$e^{i\hat{H}_S t}\hat{d}_L e^{-i\hat{H}_S t} = -e^{-i\Omega_- t}\sin(\theta/2)\hat{d}_- + e^{-i\Omega_+ t}\cos(\theta/2)\hat{d}_+, \tag{84}$$

where we used a similar notation to section 2, i.e. the diagonalized Hamiltonian reads

$$\hat{H}_S = \Omega_+ \hat{d}_+^\dagger \hat{d}_+ + \Omega_- \hat{d}_-^\dagger \hat{d}_-, \tag{85}$$

where $\Omega_\pm = \bar{\Omega} \pm \sqrt{\Delta^2 + g^2}$, with $\bar{\Omega} = (\Omega_R + \Omega_L)/2$, $\Delta = (\Omega_R - \Omega_L)/2$, and $\cos(\theta) = \Delta/\sqrt{\Delta^2 + g^2}$. Comparing equation (84), and their Hermitian conjugates, to equation (51), we find the transition frequencies

$$\{\omega_j\} = \{\Omega_+, \Omega_-, -\Omega_+, -\Omega_-\}, \tag{86}$$

and the corresponding jump operators

$$\{\hat{S}_{R,-1;j}\} = \{\sin(\theta/2)\hat{d}_+, \cos(\theta/2)\hat{d}_-, 0, 0\},$$
$$\{\hat{S}_{L,-1;j}\} = \{\cos(\theta/2)\hat{d}_+, -\sin(\theta/2)\hat{d}_-, 0, 0\},$$
$$\{\hat{S}_{R,1;j}\} = \{0, 0, \sin(\theta/2)\hat{d}_+^\dagger, \cos(\theta/2)\hat{d}_-^\dagger\},$$
$$\{\hat{S}_{L,1;j}\} = \{0, 0, \cos(\theta/2)\hat{d}_+^\dagger, -\sin(\theta/2)\hat{d}_-^\dagger\}. \tag{87}$$

We note that the frequencies $\Omega_\pm$ only feature in the jump operators with $k = -1$ (corresponding to electrons leaving the system), while the frequencies $-\Omega_\pm$ only feature in the jump operators with $k = 1$ (corresponding to electrons entering the system). This implies that we may consider only the frequencies $\Omega_\pm$ when deciding how to group the transition frequencies into sets. We may group Ω_+ and Ω_- in the same set, or we may assign them to different sets. For the frequencies $-\Omega_\pm$, we then choose an equivalent grouping.

4.2. Global approach

Grouping $\Omega_\pm$ into different sets is justified as long as their difference $2\sqrt{\Delta^2 + g^2}$ is much larger than $\max\{\kappa_L, \kappa_R\}$, which corresponds to $1/\tau_S$. This grouping results in a different set for each frequency, such that $\{\omega_q\} = \{\omega_j\}$ and $\{\hat{S}_{\alpha,k;q}\} = \{\hat{S}_{\alpha,k;j}\}$. Having identified the set frequencies and jump operators, we may then use equation (67) to obtain the well-known dissipator in the secular approximation

$$\mathcal{L}_\alpha^g = \sum_{\sigma=\pm} \kappa_\alpha^\sigma \left\{ n_F^\alpha(\Omega_\sigma)\mathcal{D}[\hat{d}_\sigma^\dagger] + [1 - n_F^\alpha(\Omega_\sigma)]\mathcal{D}[\hat{d}_\sigma] \right\}, \tag{88}$$

with the coupling strengths

$$\kappa_L^+ = \kappa_L \cos^2(\theta/2), \quad \kappa_L^- = \kappa_L \sin^2(\theta/2), \quad \kappa_R^+ = \kappa_R \sin^2(\theta/2), \quad \kappa_R^- = \kappa_R \cos^2(\theta/2). \quad (89)$$

As the jump operators in equation (87) are ladder operators of $\hat{H}_S$, no rescaling is required for obtaining the thermodynamic Hamiltonian and we find $\hat{H}_{TD} = \hat{H}_S$, resulting in the standard definition for heat currents (cf equation (70)).

4.3. Local approach

Alternatively, we may group Ω_+ and Ω_- in the same set. In this case, we need to choose a set frequency. The average value $\bar{\Omega}$ is a natural choice. Using the same arguments that result in equation (81), this grouping is justified as long as $2\sqrt{\Delta^2 + g^2} \ll \max\{k_B T_\beta, |\omega_j - \mu_\beta|\}$. In this case, we end up with two sets with the set frequencies

$$\{\omega_q\} = \{\bar{\Omega}, -\bar{\Omega}\}, \quad (90)$$

and the jump operators

$$\{\hat{S}_{R,-1;q}\} = \{\hat{d}_R, 0\},$$
$$\{\hat{S}_{L,-1;q}\} = \{\hat{d}_L, 0\},$$
$$\{\hat{S}_{R,1;q}\} = \{0, \hat{d}_R^\dagger\}, \quad (91)$$
$$\{\hat{S}_{L,1;q}\} = \{0, \hat{d}_L^\dagger\},$$

which are simply obtained by adding the jump operators in equation (87) which belong to the same set. Inserting these quantities into equation (60) results in the local approach with the dissipator

$$\mathcal{L}_\alpha^l = \kappa_\alpha \left\{ n_F^\alpha(\bar{\Omega}) \mathcal{D}[\hat{d}_\alpha^\dagger] + [1 - n_F^\alpha(\bar{\Omega})] \mathcal{D}[\hat{d}_\alpha] \right\}, \quad (92)$$

for $\alpha = L, R$.

The thermodynamic Hamiltonian is obtained by rescaling all transition frequencies to their set frequency. In the present case this rescaling is obtained by $\Omega_\pm \to \bar{\Omega}$ resulting in
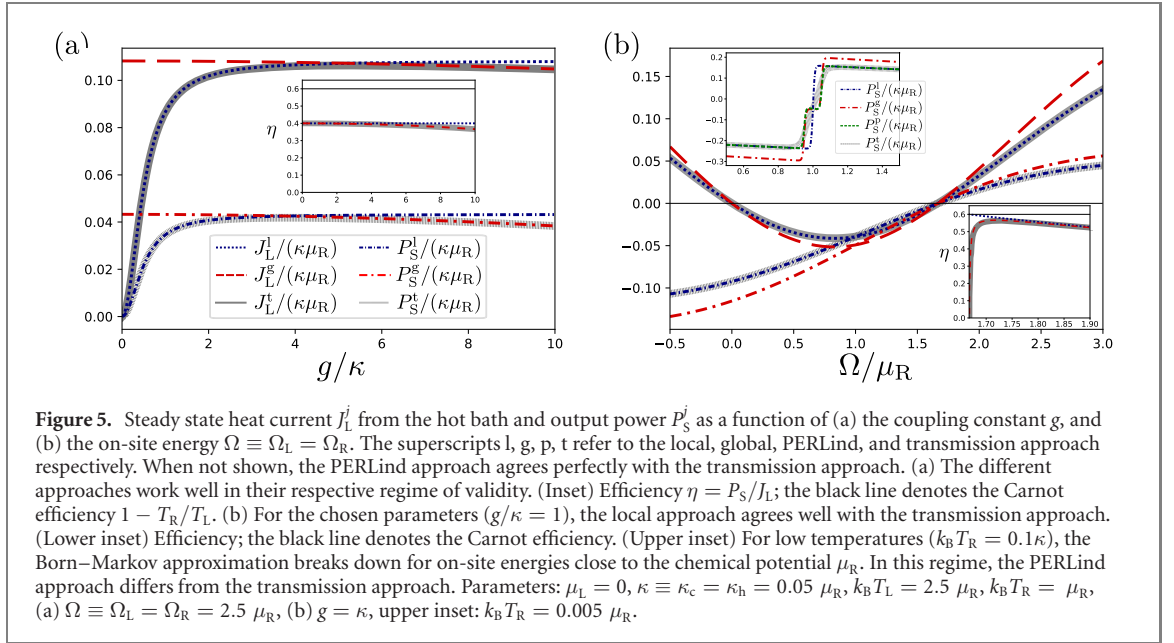
$$\hat{H}_{TD} = \bar{\Omega}(\hat{d}_+^\dagger \hat{d}_+ + \hat{d}_-^\dagger \hat{d}_-) = \bar{\Omega}(\hat{d}_L^\dagger \hat{d}_L + \hat{d}_R^\dagger \hat{d}_R). \quad (93)$$

4.4. Results

Depending on how the transition frequencies are grouped, we obtain either the global or the local approach. As long as the Born–Markov approximations are justified, i.e. as long as equation (81) holds, at least one of the two procedures is justified. As the parameters of the system are changed, we may thus need to change from the local to the global approach to maintain an adequate description of the system. This is a general drawback of our master equation: as parameters are varied, the grouping of transition frequencies into sets may need adaptation. This results in discontinuities which are expected to be small as long as the Born–Markov approximations are justified.

In figure 5, we illustrate the global, the local, as well as the benchmark provided by the transmission approach for this system when operated as a heat engine (see appendix B.2 for analytical expressions). We find that our master equation reproduces the transmission approach well if the frequency grouping is chosen such that the local (global) approach is obtained for g below (above) 5κ. Interestingly, we find that the efficiency is generally better reproduced by the global approach (see insets in figure 5). While the local approach predicts Carnot efficiency when $n_F^L(\bar{\Omega}) = n_F^R(\bar{\Omega})$, the transmission and the global approach predict a drop in efficiency. The reason for this drop is that the heat current remains finite at vanishing power when transmission occurs at more than one energy [21].

The upper inset in figure 5(b) shows that at temperatures $k_B T_\alpha \lesssim \kappa_\alpha$, the Born–Markov approximation breaks down if one of the transition frequencies $\Omega_\pm$ is close to the chemical potential μ_α, cf equation (81). In this case, the step-like behavior of the Fermi–Dirac distribution renders the assumption of a Markovian bath unjustified. By approximating transmission to occur only at the transition frequencies of the system, the Markovian master equations predict a step-like behavior of heat currents and power. The transmission approach shows that the step-like feature is smeared out by the transmission function, which is a continuous function of energy.

Figure 5. Steady state heat current J_L^j from the hot bath and output power P_S^j as a function of (a) the coupling constant g, and (b) the on-site energy $\Omega \equiv \Omega_L = \Omega_R$. The superscripts l, g, p, t refer to the local, global, PERLind, and transmission approach respectively. When not shown, the PERLind approach agrees perfectly with the transmission approach. (a) The different approaches work well in their respective regime of validity. (Inset) Efficiency $\eta = P_S/J_L$; the black line denotes the Carnot efficiency $1 - T_R/T_L$. (b) For the chosen parameters ($g/\kappa = 1$), the local approach agrees well with the transmission approach. (Lower inset) Efficiency; the black line denotes the Carnot efficiency. (Upper inset) For low temperatures ($k_B T_R = 0.1\kappa$), the Born–Markov approximation breaks down for on-site energies close to the chemical potential μ_R. In this regime, the PERLind approach differs from the transmission approach. Parameters: $\mu_L = 0$, $\kappa \equiv \kappa_c = \kappa_h = 0.05\,\mu_R$, $k_B T_L = 2.5\,\mu_R$, $k_B T_R = \mu_R$, (a) $\Omega \equiv \Omega_L = \Omega_R = 2.5\,\mu_R$, (b) $g = \kappa$, upper inset: $k_B T_R = 0.005\,\mu_R$.

5. Bosonic heat engine—a time-dependent example

5.1. System

In this section, we provide an example of a time-dependent system. To this end, we consider the heat engine introduced by Kosloff in 1984 [67] with the system Hamiltonian

$$\hat{H}_S(t) = \Omega_c \hat{a}_c^\dagger \hat{a}_c + \Omega_h \hat{a}_h^\dagger \hat{a}_h + g(\hat{a}_h^\dagger \hat{a}_c e^{-i\varpi t} + \hat{a}_c^\dagger \hat{a}_h e^{i\varpi t}), \tag{94}$$

where the bosonic annihilation and creation operators fulfill the standard commutation relations given in equation (2), and the frequency of the external drive reads

$$\varpi = \Omega_h - \Omega_{c-2\Delta}. \tag{95}$$

This Hamiltonian describes two bosonic modes with different frequencies that are coupled via a time-dependent term with a detuning quantified by Δ. For a physical implementation of this Hamiltonian based on a superconducting circuit, see reference [68]. The reservoirs and their coupling to the system are described by

$$\hat{H}_\alpha = \sum_l \varepsilon_{\alpha,l} \hat{b}_{\alpha,l}^\dagger \hat{b}_{\alpha,l}, \qquad \hat{V}_\alpha = \sum_l t_{\alpha,l}(\hat{a}_\alpha^\dagger \hat{b}_{\alpha,l} + \hat{b}_{\alpha,l}^\dagger \hat{a}_\alpha), \tag{96}$$

with $\alpha = c, h$ and we consider a vanishing chemical potential for the reservoirs, $\mu_\alpha = 0$.

From equations (50) and (96), we identify the following system and bath operators

$$\hat{S}_{\alpha,1} = \hat{a}_\alpha^\dagger, \qquad \hat{S}_{\alpha,-1} = \hat{a}_\alpha, \tag{97}$$

and

$$\hat{B}_{\alpha,1} = \sum_l t_{\alpha,l} \hat{b}_{\alpha,l}, \qquad \hat{B}_{\alpha,-1} = \sum_l t_{\alpha,l} \hat{b}_{\alpha,l}^\dagger. \tag{98}$$

We find that the Born–Markov approximations are justified when (see appendix C.1 and references [12, 13])

$$\kappa_\alpha \ll \omega_j, \tag{99}$$

where the inequality should hold for all values of α and j. This ensures that the Bose–Einstein distribution is flat around the transition energies over the energy scale κ_α. Assuming a flat bath spectral density, the same holds for the rates

$$\Gamma_1^\alpha(-\omega) = \kappa_\alpha n_B^\alpha(\omega), \qquad \Gamma_{-1}^\alpha(\omega) = \kappa_\alpha[1 - n_B^\alpha(\omega)], \tag{100}$$

where $\omega > 0$ as we are dealing with Bosons with zero chemical potential.

The time-dependence in equation (94) can be removed by a suitable unitary transformation, see reference [13], where this model was used to compare local and global master equations. Here, we use the

model to illustrate how a time-dependent Hamiltonian affects our master equation and we thus remain in the lab frame. As discussed in section 3, the average Hamiltonian defined in equation (52) is an important quantity. For our system, we find (see appendix C.2)

$$\hat{H}_{\text{av}} = \Omega_c^+ \hat{a}_+^\dagger \hat{a}_+ + \Omega_c^- \hat{a}_-^\dagger \hat{a}_-, \tag{101}$$

where the eigenmodes are given in equations (4) and (5) and we introduced the frequencies

$$\Omega_c^\pm = \Omega_c + \Delta \pm \sqrt{\Delta^2 + g^2}, \qquad \Omega_h^\pm = \Omega_h - \Delta \pm \sqrt{\Delta^2 + g^2}. \tag{102}$$

We note that this choice for the average Hamiltonian is not unique. Indeed, $\hat{H}_{\text{av}}' = \Omega_h^+ \hat{a}_+^\dagger \hat{a}_+ + \Omega_h^- \hat{a}_-^\dagger \hat{a}_-$ does also fulfill the defining relation given in equation (52).

The Fourier coefficients of the bath operators given in equation (98) are determined by

$$\hat{U}_S^\dagger(t) \hat{a}_c \hat{U}_S(t) = e^{-it\Omega_c^+} \sin(\theta/2)\hat{a}_+ + e^{-it\Omega_c^-} \cos(\theta/2)\hat{a}_-,$$
$$\hat{U}_S^\dagger(t) \hat{a}_h \hat{U}_S(t) = e^{-it\Omega_h^+} \cos(\theta/2)\hat{a}_+ - e^{-it\Omega_h^-} \sin(\theta/2)\hat{a}_-, \tag{103}$$

where θ is defined in equation (5) (where equation (95) determines Δ). From these equations (and their Hermitian conjugates) we can identify the transition rates and jump operators. As we have seen for the fermionic heat engine, it is sufficient to consider only the frequencies and operators related to particles leaving the system (the others can be treated separately and equivalently). These transition frequencies read

$$\{\omega_j\} = \{\Omega_c^+, \, \Omega_c^-, \, \Omega_h^+, \, \Omega_h^-\}. \tag{104}$$

As discussed above, these can be written as $\nu_j + l\varpi$, where ν_j denotes a transition frequency of the average Hamiltonian (i.e. $\Omega_c^\pm$ for equation (101)) and $l = 0, 1$. The corresponding jump operators read

$$\{\hat{S}_{c,-1;j}\} = \{\sin(\theta/2)\hat{a}_+, \cos(\theta/2)\hat{a}_-, 0, 0\},$$
$$\{\hat{S}_{h,-1;j}\} = \{0, 0, \cos(\theta/2)\hat{a}_+, -\sin(\theta/2)\hat{a}_-\}. \tag{105}$$

5.2. Global approach

Again, we have two choices for grouping the frequencies which result in the local and global approach respectively. We may group $\Omega_\alpha^\pm$ into different sets or assign them to the same set. Grouping them into different sets results in a single frequency per set such that $\{\omega_q\} = \{\omega_j\}$ and $\{\hat{S}_{\alpha,k;q}(t)\} = \{\hat{S}_{\alpha,k;j} \exp(-i\omega_j t)\}$ (cf equation (61)). Inserting these quantities into equation (65), we find the dissipator (in the interaction picture)

$$\tilde{\mathcal{L}}_\alpha^g = \sum_{\sigma=\pm} \frac{\kappa_\alpha^\sigma}{2} \left\{ n_B^\alpha(\Omega_\alpha^\sigma)\mathcal{D}[\hat{a}_\sigma^\dagger] + [n_B^\alpha(\Omega_\alpha^\sigma) + 1]\mathcal{D}[\hat{a}_\sigma] \right\}, \tag{106}$$

with κ_α^σ being defined in equation (22). As outlined in appendix A, a single-thermodynamic Hamiltonian is usually not sufficient for the time-dependent scenario. Furthermore, even when a secular approximation is performed, a rescaling needs to be performed [62]. In the present case, the rescaling is obtained starting from $\hat{H}_{\text{av}}$ in equation (101) and rescaling the relevant transition frequencies to ω_q. It turns out that it is sufficient to consider two thermodynamic Hamiltonians, one for each reservoir
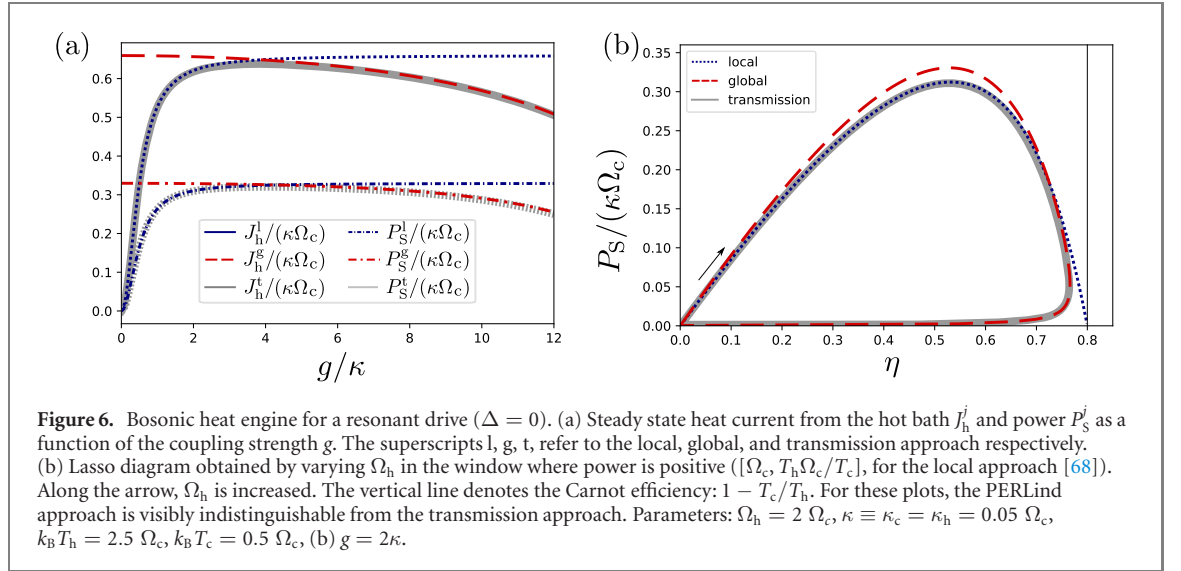
$$\hat{H}_{\text{TD}}^\alpha = \Omega_\alpha^+ \hat{a}_+^\dagger \hat{a}_+ + \Omega_\alpha^- \hat{a}_-^\dagger \hat{a}_-. \tag{107}$$

The expression for the heat current given in equation (A.5) then reduces to

$$J_\alpha = \text{Tr}\{\hat{H}_{\text{TD}}^\alpha \tilde{\mathcal{L}}_\alpha^g \hat{\rho}_S\}. \tag{108}$$

Note that the two thermodynamic Hamiltonians correspond to two possible choices for $\hat{H}_{\text{av}}$.

In this scenario, the external power can no longer be accessed by the standard expression given in equation (33). As a consequence of the secular approximation, this quantity evaluates to zero [13]. The time-averaged power can however be recovered by relying on the first law as in equation (A.6).

Figure 6. Bosonic heat engine for a resonant drive ($\Delta = 0$). (a) Steady state heat current from the hot bath J_h^j and power P_S^j as a function of the coupling strength g. The superscripts l, g, t, refer to the local, global, and transmission approach respectively. (b) Lasso diagram obtained by varying Ω_h in the window where power is positive ($[\Omega_c, T_h\Omega_c/T_c]$, for the local approach [68]). Along the arrow, Ω_h is increased. The vertical line denotes the Carnot efficiency: $1 - T_c/T_h$. For these plots, the PERLind approach is visibly indistinguishable from the transmission approach. Parameters: $\Omega_h = 2\,\Omega_c$, $\kappa \equiv \kappa_c = \kappa_h = 0.05\,\Omega_c$, $k_B T_h = 2.5\,\Omega_c$, $k_B T_c = 0.5\,\Omega_c$, (b) $g = 2\kappa$.

5.3. Local approach

Alternatively, we may group $\Omega_\alpha^\pm$ into the same set. This grouping is justified as long as $g, \Delta \ll \Omega_c, \Omega_h$ (in analogy to equation (99)). A natural choice for the set frequencies then reads

$$\{\omega_q\} = \{\Omega_c + \Delta, \Omega_h - \Delta\}, \tag{109}$$

with the jump operators

$$\{\hat{S}_{c,-1;q}(t)\} = \left\{\hat{U}_S^\dagger(t)\hat{a}_c\hat{U}_S(t), 0\right\},$$
$$\{\hat{S}_{h,-1;q}(t)\} = \left\{0, \hat{U}_S^\dagger(t)\hat{a}_h\hat{U}_S(t)\right\}. \tag{110}$$

Upon returning to the Schrödinger picture, these quantities result in the local dissipator

$$\mathcal{L}_c^l = \kappa_c\{n_B(\Omega_c + \Delta)\mathcal{D}[\hat{a}_c^\dagger] + [n_B(\Omega_c + \Delta) + 1]\mathcal{D}[\hat{a}_c]\},$$
$$\mathcal{L}_h^l = \kappa_h\{n_B(\Omega_h - \Delta)\mathcal{D}[\hat{a}_h^\dagger] + [n_B(\Omega_h - \Delta) + 1]\mathcal{D}[\hat{a}_h]\}. \tag{111}$$

Two thermodynamic Hamiltonians can again be obtained by re-scaling the transition frequencies of the average Hamiltonian in equation (101). However, due to the local structure of the jump operators, we can find a single thermodynamic Hamiltonian in the Schrödinger picture (cf appendix A)

$$\hat{H}_{TD} = (\Omega_c + \Delta)\hat{a}_c^\dagger\hat{a}_c + (\Omega_h - \Delta)\hat{a}_h^\dagger\hat{a}_h. \tag{112}$$
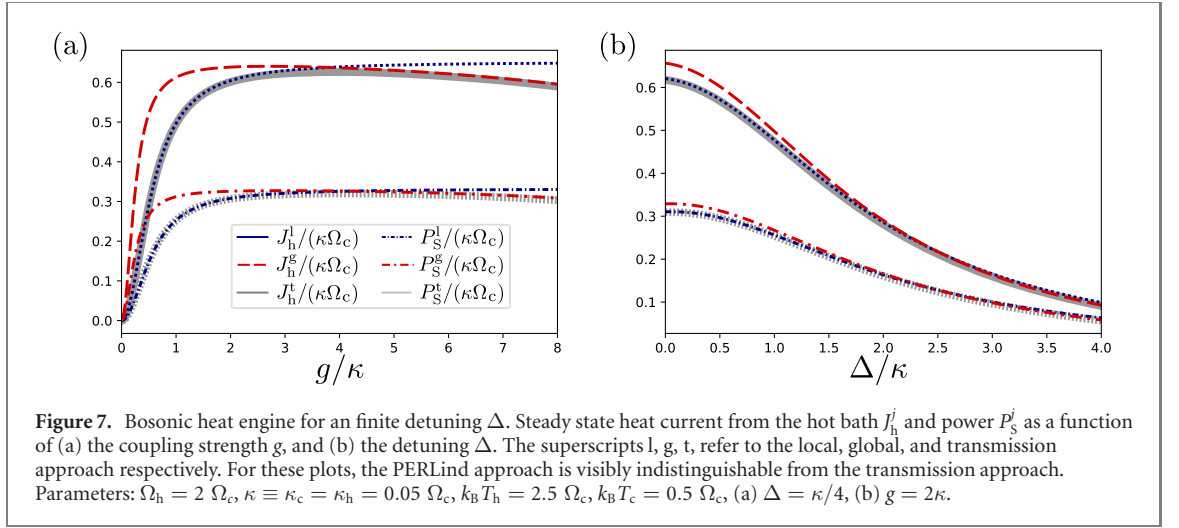
From equation (A.9), we recover the usual expression for the power produced by the system

$$P_S = -P_{ext} = i\,\mathrm{Tr}\{[\hat{H}_{TD}, \hat{H}_S(t)]\hat{\rho}_S\} = -\mathrm{Tr}\{[\partial_t\hat{H}_S(t)]\hat{\rho}_S\}. \tag{113}$$

For $\Delta = 0$, the thermodynamic Hamiltonian in equation (112) was used before in reference [56] and has an intuitive explanation: for the thermodynamic bookkeeping, we neglect the coupling energy between the bosonic modes, just as we neglect the coupling energy between system and bath.

5.4. Results

In figure 6, power, heat current, and efficiency of the bosonic heat engine for a resonant drive are illustrated. The local and global approaches for this scenario were already compared in reference [13], where exact numerics for finite reservoirs was used as a benchmark. In agreement with these results, we find that the local and global approaches together reproduce exact solutions over the full range of parameters where the Born–Markov approximation is justified. This implies that our master equation, which reduces either to the local or to the global approach, describes this scenario very well. We note that the PERLind approach reproduces the transmission approach extremely well. The disadvantage of the PERLind approach is that it is not thermodynamically consistent. The disadvantage of our master equation is that it exhibits a discontinuity when the frequency grouping is adapted (i.e. when changing from the local to the global approach).

Figure 7. Bosonic heat engine for an finite detuning Δ. Steady state heat current from the hot bath J_h^j and power P_S^j as a function of (a) the coupling strength g, and (b) the detuning Δ. The superscripts l, g, t, refer to the local, global, and transmission approach respectively. For these plots, the PERLind approach is visibly indistinguishable from the transmission approach. Parameters: $\Omega_h = 2\,\Omega_c$, $\kappa \equiv \kappa_c = \kappa_h = 0.05\,\Omega_c$, $k_B T_h = 2.5\,\Omega_c$, $k_B T_c = 0.5\,\Omega_c$, (a) $\Delta = \kappa/4$, (b) $g = 2\kappa$.

In figure 7, the performance of the heat engine at finite detuning Δ is investigated. For small detuning, we find that the global approach correctly reproduces the $g \to 0$ limit, as an exact degeneracy is no longer reached in this limit (panel (a)). As Δ increases, the low-g behavior is increasingly well captured by the global approach, because the secular approximation becomes better. For a fixed coupling strength g, we find a decrease in the heat engine performance as Δ is increased (panel (b)). This behavior is expected, because energy transfer between the drive and the system works best on resonance.

6. Interacting double quantum dot—beyond local and global approaches

6.1. System

In the previous examples, the derived master equation reduces to the well known global or local approaches. In this last example, we consider a system that has more transition frequencies, such that the master equation may differ from both the local as well as the global approach. To this end, we consider a spinless double quantum dot with Coulomb interactions described by the Hamiltonian

$$\hat{H}_S = \Omega \hat{d}_L^\dagger \hat{d}_L + \Omega \hat{d}_R^\dagger \hat{d}_R + g(\hat{d}_L^\dagger \hat{d}_R + \hat{d}_R^\dagger \hat{d}_L) + U \hat{d}_L^\dagger \hat{d}_L \hat{d}_R^\dagger \hat{d}_R$$

$$= \Omega_- \hat{d}_-^\dagger \hat{d}_- + \Omega_+ \hat{d}_+^\dagger \hat{d}_+ + U \hat{d}_-^\dagger \hat{d}_- \hat{d}_+^\dagger \hat{d}_+. \tag{114}$$

Apart from the interaction term, the system as well as the bath properties are identical to section 4 (with $\Omega \equiv \Omega_L = \Omega_R$ and $\Omega_\pm = \Omega \pm g$) where all notation used in this section is defined. From equation (114), we see that the Hamiltonian is diagonal in the occupation basis of the $\pm$ modes. The transition frequencies and jump operators are obtained from the equations

$$e^{i\hat{H}_S t} \hat{d}_R e^{-i\hat{H}_S t} = \frac{e^{-i\Omega_- t}}{\sqrt{2}}(1 - \hat{d}_+^\dagger \hat{d}_+)\hat{d}_- + \frac{e^{-i(\Omega_- + U)t}}{\sqrt{2}}\hat{d}_+^\dagger \hat{d}_+ \hat{d}_-$$

$$+ \frac{e^{-i\Omega_+ t}}{\sqrt{2}}(1 - \hat{d}_-^\dagger \hat{d}_-)\hat{d}_+ + \frac{e^{-i(\Omega_+ + U)t}}{\sqrt{2}}\hat{d}_-^\dagger \hat{d}_- \hat{d}_+,$$

$$e^{i\hat{H}_S t} \hat{d}_L e^{-i\hat{H}_S t} = -\frac{e^{-i\Omega_- t}}{\sqrt{2}}(1 - \hat{d}_+^\dagger \hat{d}_+)\hat{d}_- - \frac{e^{-i(\Omega_- + U)t}}{\sqrt{2}}\hat{d}_+^\dagger \hat{d}_+ \hat{d}_-$$

$$+ \frac{e^{-i\Omega_+ t}}{\sqrt{2}}(1 - \hat{d}_-^\dagger \hat{d}_-)\hat{d}_+ + \frac{e^{-i(\Omega_+ + U)t}}{\sqrt{2}}\hat{d}_-^\dagger \hat{d}_- \hat{d}_+. \tag{115}$$

Considering only transition frequencies that correspond to particles leaving the system, we find

$$\{\omega_j\} = \{\Omega_-, \Omega_+, \Omega_- + U, \Omega_+ + U\}, \tag{116}$$

and the jump operators

$$\{\hat{S}_{\mathrm{R},-1;j}\} = \left\{ \frac{1 - \hat{d}_+^\dagger \hat{d}_+}{\sqrt{2}} \hat{d}_-, \; \frac{1 - \hat{d}_-^\dagger \hat{d}_-}{\sqrt{2}} \hat{d}_+, \; \frac{\hat{d}_+^\dagger \hat{d}_+}{\sqrt{2}} \hat{d}_-, \; \frac{\hat{d}_-^\dagger \hat{d}_-}{\sqrt{2}} \hat{d}_+ \right\},$$

$$\{\hat{S}_{\mathrm{L},-1;j}\} = \left\{ -\frac{1 - \hat{d}_+^\dagger \hat{d}_+}{\sqrt{2}} \hat{d}_-, \; \frac{1 - \hat{d}_-^\dagger \hat{d}_-}{\sqrt{2}} \hat{d}_+, \; -\frac{\hat{d}_+^\dagger \hat{d}_+}{\sqrt{2}} \hat{d}_-, \; \frac{\hat{d}_-^\dagger \hat{d}_-}{\sqrt{2}} \hat{d}_+ \right\}.$$

(117)

6.2. Global approach
In the global approach, we choose a different set for each transition frequency. This results in the dissipator

$$\mathcal{L}_\alpha^{\mathrm{g}} = \sum_{\sigma=\pm} \frac{\kappa_\alpha}{2} \left\{ n_{\mathrm{F}}^\alpha(\Omega_\sigma) \mathcal{D}[(1 - \hat{d}_{\bar\sigma}^\dagger \hat{d}_{\bar\sigma}) \hat{d}_\sigma^\dagger] + [1 - n_{\mathrm{F}}^\alpha(\Omega_\sigma)] \mathcal{D}[(1 - \hat{d}_{\bar\sigma}^\dagger \hat{d}_{\bar\sigma}) \hat{d}_\sigma] \right.$$

$$\left. \times n_{\mathrm{F}}^\alpha(\Omega_\sigma + U) \mathcal{D}[\hat{d}_{\bar\sigma}^\dagger \hat{d}_{\bar\sigma} \hat{d}_\sigma^\dagger] + [1 - n_{\mathrm{F}}^\alpha(\Omega_\sigma + U)] \mathcal{D}[\hat{d}_{\bar\sigma}^\dagger \hat{d}_{\bar\sigma} \hat{d}_\sigma] \right\},$$

(118)

where $\bar\sigma \neq \sigma$. As usual, the thermodynamic Hamiltonian in the global approach is equal to $\hat{H}_{\mathrm{S}}$. This frequency grouping is justified when

$$|\omega_j - \omega_{j'}| \gg \kappa_\alpha,$$

(119)

for all j, j', and α.

6.3. Local approach
In the local approach, we group all transition frequencies into a single set. A natural set frequency is then the average frequency $\omega_q = \Omega + U/2$. The jump operators are given by summing the jump operators in equation (117) over j, which results in the local dissipator

$$\mathcal{L}_\alpha^{\mathrm{l}} = \kappa_\alpha \left\{ n_{\mathrm{F}}^\alpha(\Omega + U/2) \mathcal{D}[\hat{d}_\alpha^\dagger] + [1 - n_{\mathrm{F}}^\alpha(\Omega + U/2)] \mathcal{D}[\hat{d}_\alpha] \right\}.$$

(120)

The thermodynamic Hamiltonian, obtained by rescaling all transitions to $\Omega + U/2$, is given by

$$\hat{H}_{\mathrm{TD}} = (\Omega + U/2)(\hat{d}_{\mathrm{L}}^\dagger \hat{d}_{\mathrm{L}} + \hat{d}_{\mathrm{R}}^\dagger \hat{d}_{\mathrm{R}}) = (\Omega + U/2)(\hat{d}_+^\dagger \hat{d}_+ + \hat{d}_-^\dagger \hat{d}_-).$$

(121)

We note that apart from the choice of the transition frequency, the dissipator and thermodynamic Hamiltonian are identical to the one obtained for $U = 0$, cf equations (92) and (93). The frequency grouping for the local approach is justified as long as

$$|n_{\mathrm{F}}^\alpha(\omega_j) - n_{\mathrm{F}}^\alpha(\omega_{j'})| \ll 1,$$

(122)

for all j, j', and α.

6.4. Semi-local approach
In addition to the local and global approaches, we consider the low-g frequency grouping, where $\Omega_\pm$ can be replaced by Ω. This results in the set frequencies
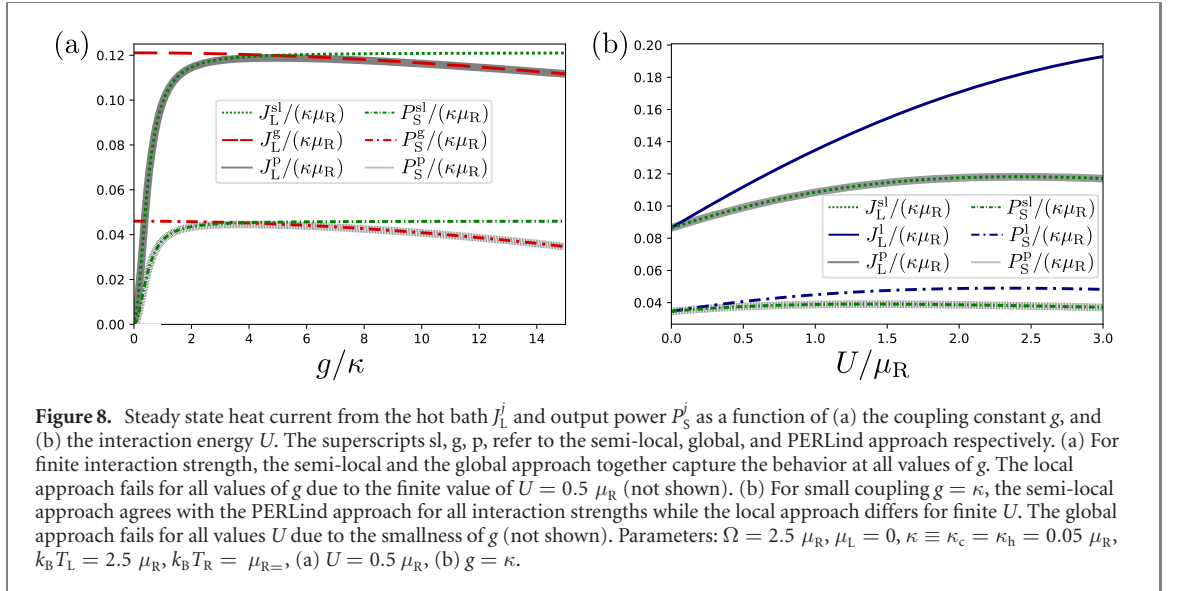
$$\{\omega_q\} = \{\Omega, \; \Omega + U\},$$

(123)

with the corresponding jump operators

$$\{\hat{S}_{\mathrm{R},-1;q}\} = \left\{ (1 - \hat{d}_{\mathrm{L}}^\dagger \hat{d}_{\mathrm{L}}) \hat{d}_{\mathrm{R}}, \; \hat{d}_{\mathrm{L}}^\dagger \hat{d}_{\mathrm{L}} \hat{d}_{\mathrm{R}} \right\},$$

$$\{\hat{S}_{\mathrm{L},-1;q}\} = \left\{ (1 - \hat{d}_{\mathrm{R}}^\dagger \hat{d}_{\mathrm{R}}) \hat{d}_{\mathrm{L}}, \; \hat{d}_{\mathrm{R}}^\dagger \hat{d}_{\mathrm{R}} \hat{d}_{\mathrm{L}} \right\}.$$

(124)

Note that the jump operators still locally change the number of electrons. However, the jumps are now dependent on the occupancy of the other dot due to the Coulomb interaction. Inserting these quantities into equation (60) results in the dissipator

$$\mathcal{L}_\alpha^{\mathrm{sl}} = \kappa_\alpha \left\{ n_{\mathrm{F}}^\alpha(\Omega) \mathcal{D}[(1 - \hat{d}_{\bar\alpha}^\dagger \hat{d}_{\bar\alpha}) \hat{d}_\alpha^\dagger] + [1 - n_{\mathrm{F}}^\alpha(\Omega)] \mathcal{D}[(1 - \hat{d}_{\bar\alpha}^\dagger \hat{d}_{\bar\alpha}) \hat{d}_\alpha] \right.$$

$$\left. + n_{\mathrm{F}}^\alpha(\Omega + U) \mathcal{D}[\hat{d}_{\bar\alpha}^\dagger \hat{d}_{\bar\alpha} \hat{d}_\alpha^\dagger] + [1 - n_{\mathrm{F}}^\alpha(\Omega + U)] \mathcal{D}[\hat{d}_{\bar\alpha}^\dagger \hat{d}_{\bar\alpha} \hat{d}_\alpha] \right\},$$

(125)

Figure 8. Steady state heat current from the hot bath J_L^j and output power P_S^j as a function of (a) the coupling constant g, and (b) the interaction energy U. The superscripts sl, g, p, refer to the semi-local, global, and PERLind approach respectively. (a) For finite interaction strength, the semi-local and the global approach together capture the behavior at all values of g. The local approach fails for all values of g due to the finite value of $U = 0.5\ \mu_R$ (not shown). (b) For small coupling $g = \kappa$, the semi-local approach agrees with the PERLind approach for all interaction strengths while the local approach differs for finite U. The global approach fails for all values U due to the smallness of g (not shown). Parameters: $\Omega = 2.5\ \mu_R$, $\mu_L = 0$, $\kappa \equiv \kappa_c = \kappa_h = 0.05\ \mu_R$, $k_B T_L = 2.5\ \mu_R$, $k_B T_R = \mu_{R=}$, (a) $U = 0.5\ \mu_R$, (b) $g = \kappa$.

where $\bar\alpha \neq \alpha$. The thermodynamic Hamiltonian corresponding to this frequency grouping reads

$$\hat H_{TD} = \Omega(\hat d_L^\dagger \hat d_L + \hat d_R^\dagger \hat d_R) + U\hat d_L^\dagger \hat d_L \hat d_R^\dagger \hat d_R. \tag{126}$$

This frequency grouping is justified for

$$|n_F^\alpha(\Omega_+) - n_F^\alpha(\Omega_-)| \ll 1, \quad \text{and} \quad |n_F^\alpha(\Omega_+ + U) - n_F^\alpha(\Omega_- + U)| \ll 1. \tag{127}$$

To ensure that the frequencies in different sets obey $|\omega_j - \omega_{j'}| \gg \kappa_\alpha$, one may expect the additional condition $U \gg g, \kappa_\alpha$. However, because no coherences can build up between states with a different total number of electrons in the system, this additional condition is not required. The semi-local approach thus enjoys a strictly larger regime of validity than the local approach (cf equation (122)), remaining valid even for a vanishing interaction strength $U = 0$.

6.5. Results
Due to the interaction term, the transmission approach no longer applies. As a benchmark, we instead use the PERLind approach, see appendix D. As mentioned above, this approach is expected to provide accurate results whenever the Born–Markov approximations are justified, an expectation that was confirmed in the examples we considered above.

Figure 8 illustrates heat current and power in the interacting double quantum dot. We find that at finite interaction strengths, the semi-local approach should be employed instead of the local approach for small coupling g. In particular, comparing figure 8(a) with figure 5(a) we find a very similar interplay between the semi-local and global approach at $U \neq 0$ as we observed between the local and global approaches for $U = 0$. We furthermore find that the semi-local approach agrees with the PERLind approach for any value of the interaction strength, as long as the coupling g is sufficiently small to respect equation (127), see figure 8(b). These results highlight the importance to go beyond the local and global approaches for systems that have more than two competing transition frequencies.

7. Conclusions

Markovian master equations in GKLS form are approximate descriptions for the reduced system state. The approximations involved in deriving these equations may not preserve the laws of thermodynamics (as is the case, e.g. in the PERLind approach). A comparison to the transmission approach for non-interacting particles illustrates that the source of any thermodynamic inconsistency is an inconsistent assignment of heat to the different jump operators appearing in the master equation. To shed light on this issue, we performed a microscopic derivation of the probability distribution for heat, employing the same approximations that are used for deriving master equations in GKLS form. We found that, when employing master equations, the resolution in heat is limited by the approximations that are performed. Exploiting this limited resolution, we derived a thermodynamically consistent master equation. To this end, we adapted the thermodynamic bookkeeping to enforce a consistent assignment of heat to the jump operators. The changes

in heat induced by this procedure remain smaller than the resolution that the master equation allows for and are thus consistent with the performed approximations. This refined thermodynamic bookkeeping is captured by a thermodynamic Hamiltonian, which may differ from the Hamiltonian that determines the dynamics of the quantum state.

We illustrated our master equation with three different examples, including a time-dependent model and a model that includes interactions. Our master equation may reduce to the well-known global approach, or to a thermodynamically consistent version of the local approach in their respective regime of validity. For systems where neither of these approaches is adequate, it provides a novel description.

Our master equation provides a thermodynamically consistent description for quantum systems that are amenable to a Markovian description. This allows future investigations on the thermodynamics of quantum devices to fully rely on the conclusions that follow from basic thermodynamics.

Acknowledgments

Data availability statement

All data that support the findings of this study are included within the article (and any supplementary files).

Appendix A. Thermodynamic consistency for a time-dependent Hamiltonian

Here we show how thermodynamic consistency is obtained for a time-dependent system Hamiltonian. We note that the 0th law only applies to the time-independent scenario, as no equilibration is expected in the presence of an external drive.

Let us first consider slow driving, where $\hat{H}_S(t)$ changes on a time-scale that is much larger than the bath correlation time τ_B. In this case, a master equation may be derived by considering the Hamiltonian to be *frozen*, treating its time argument as any other parameter [69]. We may still use equation (66) but the transition frequencies ω_j and ω_q, as well as the operators $\hat{S}_{\alpha,k;j}$ become time-dependent. The thermodynamic Hamiltonian, obtained as in the time-independent case outlined in section 3.6, then also becomes time-dependent and the first law reads

$$\partial_t U = \mathrm{Tr}\{(\partial_t \hat{H}_{\mathrm{TD}})\hat{\rho}\} + \sum_{\alpha}(P_\alpha + J_\alpha), \tag{A.1}$$

where the internal energy as well as the heat-current and power from reservoir α are still defined by equations (69) and (70) respectively. The first term on the right-hand side of equation (A.1) denotes the power provided by the external drive. The second law still holds as discussed in section 3.6.

Next, we consider a time-periodic system Hamiltonian with period $t_p = 2\pi/\varpi$. In this case, the frequencies ω_j are not directly transition frequencies but rather fulfill

$$\omega_{j,l} = \nu_j + l\varpi, \tag{A.2}$$

where l is an integer and ν_j are the transition frequencies of the averaged Hamiltonian $\hat{H}_{\mathrm{av}}$ defined in equation (52). For clarity, we extended the index of $\omega_{j,l}$ to explicitly include l, such that j uniquely defines the transition frequency of the averaged Hamiltonian. We stress that in this scenario, equations (59) and (64) hold. Throughout this appendix, we remain in the interaction picture, because going to the Schrödinger picture is non-trivial for time-dependent Hamiltonians (cf the comment below equation (67)). Since any time-dependence may be thought of as a single-period of a periodic process, our master equation is applicable for any time-dependence. However, for a thermodynamically consistent description, we require the additional assumption

$$\varpi \gg 1/\tau_S, \tag{A.3}$$

which is complementary to the slow driving regime discussed above. As in the time-independent case, we may group the frequencies into sets x_q, such that

$$|\omega_{j,l} - \omega_{j',l'}| \ll 1/\tau_{\rm B} \quad \text{for } \omega_{j,l} \in x_q,\ \omega_{j',l'} \in x_{q'} \text{ with } \hat{q} = \hat{q}',$$
$$|\omega_{j,l} - \omega_{j',l'}| \gg 1/\tau_{\rm S} \quad \text{for } \omega_{j,l} \in x_q,\ \omega_{j',l'} \in x_{q'} \text{ with } q \neq q'. \tag{A.4}$$

We note that due to equation (A.3), we may choose the sets x_q such that $\omega_{j,l}$ and $\omega_{j,l'}$ are not in the same set for $l \neq l'$. In that case, all frequencies in a given set have different values for j, i.e. correspond to different transition frequencies ν_j of the averaged Hamiltonian. For a given set x_q, a thermodynamic Hamiltonian $\hat{H}_{\rm TD}^q$ may be obtained by rescaling $\nu_j \rightarrow \omega_q$ for all j that occur in the set x_q. In contrast to the time-independent case, the same transition frequency ν_j may feature in different sets (as it may feature in different $\omega_{j,l}$). The rescaling therefore has to be done individually for each set. We note that this rescaling is even required in the secular approximation since ν_j and $\omega_{j,l}$ differ by $l\varpi$ [62]. The heat current from bath α, obtained from equations (59) and (36) can then be cast into

$$J_\alpha = \sum_{\{q|\omega_q>0\}} \text{Tr}\{(\hat{H}_{\rm TD}^q - \mu_\alpha \hat{N}_{\rm S})\tilde{\mathcal{L}}_{\alpha;q}\hat{\rho}_{\rm S}\}, \tag{A.5}$$

with $\tilde{\mathcal{L}}_{\alpha;q}$ given in equation (65).

To arrive at the master equation in equation (66), we dropped terms that oscillate with frequencies much larger than $1/\tau_{\rm S}$. Unfortunately, these terms may be important when evaluating the standard expression for external power given in equation (33). Loosely speaking, the oscillations of the density matrix cancel oscillations of $\partial_t \hat{H}_{\rm S}(t)$, thereby contributing to the average power. In general, one may no longer disentangle the internal energy from the external power [70]. We may then still consider the first law upon taking a long-time average, ensuring that changes in the internal energy become negligible. Similarly, one could average over a single period when the system has reached a limit cycle. The first law then reduces to

$$0 = \bar{P}_{\rm ext} + \sum_\alpha (\bar{P}_\alpha + \bar{J}_\alpha), \tag{A.6}$$

where the bar denotes any kind of average that ensures a vanishing change in internal energy.

Interestingly, one may still access the internal energy (and thus the time-dependent power) when the master equation takes on a local structure. To illustrate this, let us consider a coupling Hamiltonian of the form

$$\hat{V} = \sum_\alpha \left(\hat{S}_\alpha \hat{B}_\alpha^\dagger + \hat{B}_\alpha \hat{S}_\alpha^\dagger\right). \tag{A.7}$$

A local master equation is obtained when we group the transition frequencies such that each set frequency corresponds to a single reservoir, i.e. $\{\omega_q\} = \{\omega_\alpha\}$. In this case, the jump operators (in the interaction picture and dropping the index q) are of the form $\hat{S}_\alpha(t) = \hat{U}_{\rm S}^\dagger(t)\hat{S}_\alpha \hat{U}_{\rm S}(t)$ (cf equation (61)). For each jump operator, we then introduce a corresponding number operator $\hat{n}_\alpha$, such that $[\hat{S}_\alpha, \hat{n}_\alpha] = \hat{S}_\alpha$. In this case, we may define a single, albeit time-dependent, thermodynamic Hamiltonian (in the interaction picture)

$$\hat{H}_{\rm TD} = \sum_\alpha \omega_\alpha \hat{U}_{\rm S}^\dagger(t)\hat{n}_\alpha \hat{U}_{\rm S}(t), \tag{A.8}$$

which fulfills the defining property $[\hat{S}_\alpha(t), \hat{H}_{\rm TD}] = \omega_\alpha \hat{S}_\alpha(t)$. One may then still use equation (69) to define the internal energy and the first law reads

$$\partial_t U = -\text{i}\, \text{Tr}\{[\hat{H}_{\rm TD}, \hat{H}_{\rm S}(t)]\hat{\rho}_{\rm S}\} + \sum_\alpha (P_\alpha + J_\alpha), \tag{A.9}$$

which is valid both in the interaction, as well as in the Schrödinger picture where both the jump operators as well as the thermodynamic Hamiltonian become time-independent. The first term on the right-hand side of equation (A.9) can be identified with the power provided by the external drive.

To verify the second law, we write the entropy production rate as

$$\dot{\Sigma} = -k_{\rm B}\sum_\alpha \sum_{\{q|\omega_q>0\}} \text{Tr}\{(\tilde{\mathcal{L}}_{\alpha;q}\hat{\rho}_{\rm S})[\ln\hat{\rho}_{\rm S} - \ln\hat{\rho}_{\rm G}^q]\} \geqslant 0, \tag{A.10}$$

where we introduced

$$\hat{\rho}_{\rm G}^q = \frac{e^{-\beta(\hat{H}_{\rm TD}^q - \mu\hat{N}_{\rm S})}}{\text{Tr}\{e^{-\beta(\hat{H}_{\rm TD}^q - \mu\hat{N}_{\rm S})}\}}. \tag{A.11}$$

Spohns inequality ensures the positivity of the entropy production rate since $\tilde{\mathcal{L}}_{\alpha;q}\hat{\rho}_{\rm G}^q = 0$.

Appendix B. Supplemental calculations for the fermionic heat engine

B.1. Bath correlation functions

The bath operators given in equation (80) result in the bath correlation functions (cf equation (55))

$$
C_1^\alpha = \frac{\kappa_\alpha}{2} e^{is\mu_\alpha} \left[\delta(s) - i \frac{k_B T_\alpha}{\sinh(\pi s k_B T_\alpha)} \right],
$$
$$
C_{-1}^\alpha = \frac{\kappa_\alpha}{2} e^{-is\mu_\alpha} \left[\delta(s) - i \frac{k_B T_\alpha}{\sinh(\pi s k_B T_\alpha)} \right],
$$
(B.1)

where we introduced the bath spectral density

$$
\frac{\kappa_\alpha}{2\pi} = \sum_l t_{\alpha,l}^2 \delta(\omega - \varepsilon_{\alpha,l}),
$$
(B.2)

quantifying the system-bath coupling and which we assume to be constant as a function of ω. We note that $C_k^\alpha \equiv C_{k,k}^\alpha$ and $C_{k,k'}^\alpha \propto \delta_{k,k'}$. The bath correlation functions decay on the time-scale β_α. The bath correlation time can thus be identified by $\tau_B = \max\{\beta_L, \beta_R\}$. The system (in the interaction picture) changes on the time-scale $\tau_S = \min\{1/\kappa_L, 1/\kappa_R\}$. Thus, the Born–Markov approximations are expected to hold for temperatures that are much higher than the coupling between system and bath. Furthermore, from the Redfield equation in equation (53), together with equation (B.1), we find that the integral over s involves factors $\exp[is(\omega_j \pm \mu_\alpha)]$. Whenever $|\omega_j \pm \mu_\alpha| \gg k_B T_\alpha$, the rapid oscillations of these factors imply that only values of $s \lesssim 1/(\omega_j \pm \mu_\alpha)$ contribute to the integral. For larger values of s, the term $k_B T_\alpha / \sinh(\pi s k_B T_\alpha)$ varies on a time-scale much slower than the oscillations. This implies that the Born–Markov approximations are also justified in the regime $|\omega_j \pm \mu_\alpha| \gg k_B T_\alpha$ and $\min\{|\omega_j \pm \mu_L|, |\omega_j \pm \mu_R|\} \gg 1/\tau_S$. Now in case $1/\tau_S \ll |\omega_j \pm \mu|$ (dropping the bath index for ease of notation), either we have $k_B T \ll |\omega_j \pm \mu|$, such that the Born–Markov approximations are justified, or we have $k_B T \gtrsim |\omega_j \pm \mu|$ which implies $1/\tau_S \ll k_B T$, also ensuring the Born–Markov approximation. In the first case, the bath-correlation functions oscillate to zero over times much smaller than τ_S, in the latter case the bath correlation functions decay much faster than τ_S. As a consequence, the Born–Markov approximations are fulfilled whenever κ is much smaller than either $k_B T$, or $|\omega_j \pm \mu|$ as expressed in equation (81).

The Fourier transforms of the bath correlation functions are given by equation (82). We reach the same conclusions about the validity of the Born–Markov approximation by demanding that these functions are flat over the energy scale κ (the inverse of τ_S). For $\kappa \ll k_B T$, the Fermi–Dirac distribution is everywhere slowly varying compared to κ. For $\kappa \ll |\omega - \mu|$ and $k_B T \ll |\omega - \mu|$, the Fermi function is either very close to zero or one, depending on the sign of $\omega - \mu$, and remains so over the energy scale of κ.

B.2. Power and heat currents

For the double dot system with non-interacting fermions the Landauer-like formula provides the following steady state heat current (out of the left lead)

$$
J_L^t = \frac{1}{2\pi} \int_{-\infty}^{\infty} d\omega \, \mathcal{T}(\omega)(\omega - \mu_L)[n_F^L(\omega) - n_F^R(\omega)],
$$
(B.3)

and power

$$
P_S^t = \frac{(\mu_R - \mu_L)}{2\pi} \int_{-\infty}^{\infty} d\omega \, \mathcal{T}(\omega)[n_F^L(\omega) - n_F^R(\omega)],
$$
(B.4)

with the transmission function

$$
\mathcal{T}(\omega) = \frac{g^2 \kappa_L \kappa_R}{\left| \left(\omega - \Omega_L + i\frac{\kappa_L}{2} \right) \left(\omega - \Omega_R + i\frac{\kappa_R}{2} \right) - g^2 \right|^2}.
$$
(B.5)

Note that the transmission function is the same as for the bosonic system, cf equation (10).

For the global and local approaches, the definitions for the heat current and the power are given in equations (70) and (71), with $\hat{N}_S = \hat{d}_L^\dagger \hat{d}_L + \hat{d}_R^\dagger \hat{d}_R$. For the local approach, we find

$$
J_L^l = \frac{(\bar{\Omega} - \mu_L)}{\kappa_L + \kappa_R} \frac{4g^2 \kappa_L \kappa_R [n_F^L(\bar{\Omega}) - n_F^R(\bar{\Omega})]}{4g^2 + \kappa_L \kappa_R + 16\Delta^2 \kappa_L \kappa_R / (\kappa_L + \kappa_R)^2},
$$
(B.6)

and

$$
P_S^l \equiv -P_L^l - P_R^l = \frac{(\mu_R - \mu_L)}{(\bar{\Omega} - \mu_L)} J^l.
$$
(B.7)

This tight-coupling condition between heat current and power (which can be inferred from the form of $\hat{H}_{\text{TD}}$, cf equation (93)) is a direct result of approximating transmission to happen at a single energy.

For the global approach, we find

$$J_{\text{L}}^{\text{g}} = \sum_{\sigma=\pm} (\Omega_\sigma - \mu_{\text{L}}) \frac{\kappa_{\text{L}}^\sigma \kappa_{\text{R}}^\sigma}{\kappa_{\text{L}}^\sigma + \kappa_{\text{R}}^\sigma} [n_{\text{F}}^{\text{L}}(\Omega_\sigma) - n_{\text{F}}^{\text{R}}(\Omega_\sigma)], \tag{B.8}$$

and

$$P_{\text{S}}^{\text{g}} \equiv -P_{\text{L}}^{\text{g}} - P_{\text{R}}^{\text{g}} = (\mu_{\text{R}} - \mu_{\text{L}}) \sum_{\sigma=\pm} \frac{\kappa_{\text{L}}^\sigma \kappa_{\text{R}}^\sigma}{\kappa_{\text{L}}^\sigma + \kappa_{\text{R}}^\sigma} [n_{\text{F}}^{\text{L}}(\Omega_\sigma) - n_{\text{F}}^{\text{R}}(\Omega_\sigma)]. \tag{B.9}$$

Finally, in the PERLind approach the dissipators read

$$\mathcal{L}_\alpha^{\text{p}} = \sum_{k=-1,1} \mathcal{D}[\hat{J}_{\alpha,k}], \tag{B.10}$$

with the jump operators

$$\begin{aligned}
\hat{J}_{\text{R},-1} &= \sqrt{\kappa_{\text{R}}^+ [1 - n_{\text{F}}^{\text{R}}(\Omega_+)]} \hat{d}_+ + \sqrt{\kappa_{\text{R}}^- [1 - n_{\text{F}}^{\text{R}}(\Omega_-)]} \hat{d}_-, \\
\hat{J}_{\text{R},1} &= \sqrt{\kappa_{\text{R}}^+ n_{\text{F}}^{\text{R}}(\Omega_+)} \hat{d}_+^\dagger + \sqrt{\kappa_{\text{R}}^- n_{\text{F}}^{\text{R}}(\Omega_-)} \hat{d}_-^\dagger, \\
\hat{J}_{\text{L},-1} &= \sqrt{\kappa_{\text{L}}^+ [1 - n_{\text{F}}^{\text{L}}(\Omega_+)]} \hat{d}_+ - \sqrt{\kappa_{\text{L}}^- [1 - n_{\text{F}}^{\text{L}}(\Omega_-)]} \hat{d}_-, \\
\hat{J}_{\text{L},1} &= \sqrt{\kappa_{\text{L}}^+ n_{\text{F}}^{\text{L}}(\Omega_+)} \hat{d}_+^\dagger - \sqrt{\kappa_{\text{L}}^- n_{\text{F}}^{\text{L}}(\Omega_-)} \hat{d}_-^\dagger.
\end{aligned} \tag{B.11}$$

In this approach, heat current and power are defined as

$$J_{\text{L}}^{\text{p}} = \text{Tr} \left\{ (\hat{H}_{\text{S}} - \mu_{\text{L}} \hat{N}_{\text{S}}) \mathcal{L}_{\text{L}}^{\text{p}} \hat{\rho} \right\}, \tag{B.12}$$

and

$$P_{\text{S}}^{\text{p}} = -\mu_{\text{L}} \, \text{Tr} \left\{ \hat{N}_{\text{S}} \mathcal{L}_{\text{L}}^{\text{p}} \hat{\rho} \right\} - \mu_{\text{R}} \, \text{Tr} \left\{ \hat{N}_{\text{S}} \mathcal{L}_{\text{R}}^{\text{p}} \hat{\rho} \right\}. \tag{B.13}$$

Appendix C. Supplemental calculations for the bosonic heat engine

C.1. Bath correlations functions
The bath operators in equation (98) result in the bath correlation functions (cf equation (55))

$$\begin{aligned}
C_1^\alpha &= \int_0^\infty \frac{d\omega}{2\pi} \kappa_\alpha e^{is\omega} n_{\text{B}}^\alpha(\omega), \\
C_{-1}^\alpha &= \int_0^\infty \frac{d\omega}{2\pi} \kappa_\alpha e^{-is\omega} [n_{\text{B}}^\alpha(\omega) + 1],
\end{aligned} \tag{C.1}$$

where κ_α is given by equation (B.2) and we have $C_k^\alpha \equiv C_{k,k}^\alpha$ and $C_{k,k'}^\alpha \propto \delta_{k,k'}$. We note that these integrals only converge if $\kappa_\alpha \to 0$ for $\omega \to 0$. Here we do not give a specific form of κ_α and directly proceed to investigating the Fourier transforms of the bath correlation functions. For a detailed discussion on the bath correlation functions for an ohmic spectral density, we refer to reference [12]. By Fourier transforming equation (C.1), we find the rates given in equation (100). We note that even if κ_α needs to vanish as $\omega \to 0$, we can still assume it to be constant over all energies that the system probes (i.e. all energies where the transmission function is non-zero).

Similarly to the fermionic case, the Born–Markov approximations are justified when the quantities in equation (100) remain constant over the energy interval κ_α around the transition frequencies of the system. This is the case if $\kappa_\alpha \ll \omega_j$. We note that for very small temperatures ($k_{\text{B}}T \ll \omega_j$), $n_{\text{B}}(\omega_j)$ becomes exponentially small and the dynamics is dominated by the temperature-independent term in equation (100) which corresponds to spontaneous emission. We further note that $\kappa_\alpha \ll k_{\text{B}}T_\alpha$ is not a sufficient condition for the Born–Markov approximation to be justified. When $\kappa_\alpha \to \omega_j$, then $n_{\text{B}}(\omega_j - \kappa_\alpha)$ diverges, no matter the temperature. The conclusions drawn here from the Fourier transform of the bath correlation functions are in complete agreement with the conclusions obtained in reference [12] by considering the bath correlation functions for an ohmic spectral density.

C.2. The average Hamiltonian

To derive the average Hamiltonian for the system given in equation (94), we first consider the rotating frame determined by the unitary transformation

$$\hat{U}_r = e^{it[(\Omega_c + \Delta)\hat{a}_c^\dagger \hat{a}_c + (\Omega_h - \Delta)\hat{a}_h^\dagger \hat{a}_h]}. \tag{C.2}$$

In the rotating frame, we find the time-independent Hamiltonian

$$\tilde{H}_S = \hat{U}_r(t)\hat{H}_S(t)\hat{U}_r^\dagger(t) - i\hat{U}_r(t)\partial_t \hat{U}_r^\dagger(t) = \Delta(\hat{a}_h^\dagger \hat{a}_h - \hat{a}_c^\dagger \hat{a}_c) + g(\hat{a}_h^\dagger \hat{a}_c + \hat{a}_c^\dagger \hat{a}_h). \tag{C.3}$$

The time-evolution operator in the lab frame fulfills the relation

$$\hat{U}_S(t) = \mathcal{T}e^{-i\int_0^t dt' \hat{H}_S(t')} = \hat{U}_r^\dagger(t)\tilde{U}_S(t), \tag{C.4}$$

where $\tilde{U}_S(t)$ denotes the time-evolution operator for the system in the rotating frame.

To obtain the average Hamiltonian, we use the relations

$$e^{it_p \varpi \hat{n}_j} = 1, \tag{C.5}$$

for $t_p = 2\pi/\varpi$, where $\hat{n}_j$ is any operator that only has integer eigenvalues (such as a photon number operator). With the help of this relation, one can show

$$\hat{U}_S(t_p) = e^{-it_p[\Omega_\alpha^+ \hat{a}_+^\dagger \hat{a}_+ + \Omega_\alpha^- \hat{a}_-^\dagger \hat{a}_-]}, \tag{C.6}$$

which holds both for $\alpha = c, h$ (the frequencies are given in equation (102)), resulting in the two choices for the average Hamiltonian discussed in the main text.

C.3. Power and heat currents

In the rotating frame discussed in the last subsection, the bosonic heat engine looks just like the system discussed in section 2, upon setting $\bar{\Omega} = 0$ and shifting the energies of the reservoir modes by $\Omega_c + \Delta$ and $\Omega_h - \Delta$ respectively (see also reference [13]). We then obtain the Landauer-like formula for the heat current

$$J_h^t = \frac{1}{2\pi} \int_\varpi^\infty d\omega \mathcal{T}(\omega)\omega[n_B^h(\omega) - n_B^c(\omega - \varpi)], \tag{C.7}$$

and for power we find

$$P_S^t = \frac{1}{2\pi} \int_{-\Omega_c}^\infty d\omega \mathcal{T}(\omega)\varpi[n_B^h(\omega) - n_B^c(\omega - \varpi)], \tag{C.8}$$

with the transmission function

$$\mathcal{T}(\omega) = \frac{g^2 \kappa_c \kappa_h}{\left| \left(\omega - \Omega_h + i\frac{\kappa_c}{2}\right)\left(\omega - \Omega_c - \varpi + i\frac{\kappa_h}{2}\right) - g^2 \right|^2}. \tag{C.9}$$

For the local approach, we find the heat current

$$J_h^l = \frac{\Omega_h - \Delta}{\kappa_c + \kappa_h} \frac{4g^2 \kappa_c \kappa_h[n_B^h(\Omega_h - \Delta) - n_B^c(\Omega_c + \Delta)]}{4g^2 + \kappa_c \kappa_h + 16\Delta^2 \kappa_c \kappa_h/(\kappa_c + \kappa_h)^2}, \tag{C.10}$$

and power

$$P^l = \left(1 - \frac{\Omega_c + \Delta}{\Omega_h - \Delta}\right) J_h^l. \tag{C.11}$$

The global approach results in the heat current

$$J_h^g = \sum_{\sigma=\pm} \Omega_h^\sigma \frac{\kappa_c^\sigma \kappa_h^\sigma}{\kappa_c^\sigma + \kappa_h^\sigma}[n_B^h(\Omega_h^\sigma) - n_B^c(\Omega_c^\sigma)], \tag{C.12}$$

and power

$$P_S^g \equiv J_h + J_c = \sum_{\sigma=\pm} \varpi \frac{\kappa_c^\sigma \kappa_h^\sigma}{\kappa_c^\sigma + \kappa_h^\sigma}[n_B^h(\Omega_h^\sigma) - n_B^c(\Omega_c^\sigma)]. \tag{C.13}$$

Finally, for the PERLind approach, the dissipators read (in the rotating frame)

$$\mathcal{L}_\alpha^p = \sum_{k=-1,1} \mathcal{D}[\hat{J}_{\alpha,k}], \tag{C.14}$$

with the jump operators

$$\hat{J}_{c,-1} = \sqrt{\kappa_c^+ [n_B^c(\Omega_c^+) + 1]}\hat{a}_+ + \sqrt{\kappa_c^- [n_B^c(\Omega_c^-) + 1]}\hat{a}_-,$$

$$\hat{J}_{c,1} = \sqrt{\kappa_c^+ n_B^c(\Omega_c^+)}\hat{a}_+^\dagger + \sqrt{\kappa_c^- n_B^c(\Omega_c^-)}\hat{a}_-^\dagger,$$

$$\hat{J}_{h,-1} = \sqrt{\kappa_h^+ [n_B^h(\Omega_h^+) + 1]}\hat{a}_+ - \sqrt{\kappa_h^- [n_B^h(\Omega_h^-) + 1]}\hat{a}_-, \tag{C.15}$$

$$\hat{J}_{h,1} = \sqrt{\kappa_h^+ n_B^h(\Omega_h^+)}\hat{a}_+^\dagger - \sqrt{\kappa_h^- n_B^h(\Omega_g^-)}\hat{a}_-^\dagger.$$

In this approach, the heat currents can be obtained from equation (53) by applying the approximations discussed in the supplemental material of reference [30]. For the present system, we obtain

$$J_\alpha^p = \sum_{\sigma,\sigma'=\pm} \frac{\Omega_\alpha^\sigma + \Omega_\alpha^{\sigma'}}{2} \text{Tr}\left\{ \left(\hat{J}_{\alpha,1;\sigma}^\dagger \hat{J}_{\alpha,1;\sigma'} - \hat{J}_{\alpha,-1;\sigma}^\dagger \hat{J}_{\alpha,-1;\sigma'} \right) \tilde{\rho} \right\}, \tag{C.16}$$

where

$$\hat{J}_{\alpha,k} = \hat{J}_{\alpha,k;+} + \hat{J}_{\alpha,k;-}, \tag{C.17}$$

and $\hat{J}_{\alpha,k;\sigma}$ can be inferred from equation (C.15) as the term that is proportional to $\hat{a}_\sigma^{(\dagger)}$. The power is given by

$$P_S^p = J_h^p + J_c^p. \tag{C.18}$$

Appendix D. PERLind approach for the interacting double quantum dot

For the interacting double quantum dot discussed in section 6, the dissipators in the PERLind approach read

$$\mathcal{L}_\alpha^p = \sum_{k=-1,1} \mathcal{D}[\hat{J}_{\alpha,k}], \tag{D.1}$$

with the jump operators

$$\hat{J}_{R,-1} = \sqrt{\frac{\kappa_R}{2}[1 - n_F^R(\Omega_+)]}(1 - \hat{d}_-^\dagger \hat{d}_-)\hat{d}_+ + \sqrt{\frac{\kappa_R}{2}[1 - n_F^R(\Omega_+ + U)]}\hat{d}_-^\dagger \hat{d}_- \hat{d}_+ +$$

$$+ \sqrt{\frac{\kappa_R}{2}[1 - n_F^R(\Omega_-)]}(1 - \hat{d}_+^\dagger \hat{d}_+)\hat{d}_- + \sqrt{\frac{\kappa_R}{2}[1 - n_F^R(\Omega_- + U)]}\hat{d}_+^\dagger \hat{d}_+ \hat{d}_-,$$

$$\hat{J}_{R,1} = \sqrt{\frac{\kappa_R}{2}n_F^R(\Omega_+)}(1 - \hat{d}_-^\dagger \hat{d}_-)\hat{d}_+^\dagger + \sqrt{\frac{\kappa_R}{2}n_F^R(\Omega_+ + U)}\hat{d}_-^\dagger \hat{d}_- \hat{d}_+^\dagger +$$

$$+ \sqrt{\frac{\kappa_R}{2}n_F^R(\Omega_-)}(1 - \hat{d}_+^\dagger \hat{d}_+)\hat{d}_-^\dagger + \sqrt{\frac{\kappa_R}{2}n_F^R(\Omega_- + U)}\hat{d}_+^\dagger \hat{d}_+ \hat{d}_-^\dagger,$$

$$\hat{J}_{L,-1} = \sqrt{\frac{\kappa_L}{2}[1 - n_F^L(\Omega_+)]}(1 - \hat{d}_-^\dagger \hat{d}_-)\hat{d}_+ + \sqrt{\frac{\kappa_L}{2}[1 - n_F^L(\Omega_+ + U)]}\hat{d}_-^\dagger \hat{d}_- \hat{d}_+ +$$

$$- \sqrt{\frac{\kappa_L}{2}[1 - n_F^L(\Omega_-)]}(1 - \hat{d}_+^\dagger \hat{d}_+)\hat{d}_- - \sqrt{\frac{\kappa_L}{2}[1 - n_F^L(\Omega_- + U)]}\hat{d}_+^\dagger \hat{d}_+ \hat{d}_-,$$

$$\hat{J}_{L,1} = \sqrt{\frac{\kappa_L}{2}n_F^L(\Omega_+)}(1 - \hat{d}_-^\dagger \hat{d}_-)\hat{d}_+^\dagger + \sqrt{\frac{\kappa_L}{2}n_F^L(\Omega_+ + U)}\hat{d}_-^\dagger \hat{d}_- \hat{d}_+^\dagger +$$

$$- \sqrt{\frac{\kappa_L}{2}n_F^L(\Omega_-)}(1 - \hat{d}_+^\dagger \hat{d}_+)\hat{d}_-^\dagger - \sqrt{\frac{\kappa_L}{2}n_F^L(\Omega_- + U)}\hat{d}_+^\dagger \hat{d}_+ \hat{d}_-^\dagger. \tag{D.2}$$

ORCID iDs

Patrick P Potts ⓘ https://orcid.org/0000-0001-6036-7291
Alex Arash Sand Kalaee ⓘ https://orcid.org/0000-0003-2691-724X
Andreas Wacker ⓘ https://orcid.org/0000-0003-1758-6274

References

[1] Breuer H-P and Petruccione F 2002 *The Theory of Open Quantum Systems* (Oxford: Oxford University Press)
[2] Weiss U 1993 *Quantum Dissipative Systems* (Singapore: World Scientific)
[3] Kamenev A 2011 *Field Theory of Non-equilibrium Systems* (Cambridge: Cambridge University Press)
[4] Schaller G 2014 *Open Quantum Systems Far from Equilibrium* (Berlin: Springer)
[5] Gorini V, Kossakowski A and Sudarshan E C G 1976 Completely positive dynamical semigroups of N-level systems *J. Math. Phys.* **17** 821
[6] Lindblad G 1976 On the generators of quantum dynamical semigroups *Commun. Math. Phys.* **48** 119
[7] Dann R, Levy A and Kosloff R 2018 Time-dependent Markovian quantum master equation *Phys. Rev. A* **98** 052129
[8] Carmichael H 1991 *An Open Systems Approach to Quantum Optics* (Berlin: Springer)
[9] Restrepo J, Ciuti C and Favero I 2014 Single-polariton optomechanics *Phys. Rev. Lett.* **112** 013601
[10] Cresser J D 1992 Thermal equilibrium in the Jaynes–Cummings model *J. Mod. Opt.* **39** 2187
[11] Scala M, Militello B, Messina A, Piilo J and Maniscalco S 2007 Microscopic derivation of the Jaynes–Cummings model with cavity losses *Phys. Rev. A* **75** 013811
[12] Rivas Á, Plato A D K, Huelga S F and Plenio M B 2010 Markovian master equations: a critical study *New J. Phys.* **12** 113032
[13] Hofer P P, Perarnau-Llobet M, Miranda L D M, Haack G, Silva R, Brask J B and Brunner N 2017 Markovian master equations for quantum thermal machines: local versus global approach *New J. Phys.* **19** 123037
[14] González J O, Correa L A, Nocerino G, Palao J P, Alonso D and Adesso G 2017 Testing the validity of the 'local' and 'global' GKLS master equations on an exactly solvable model *Open Syst. Inf. Dyn.* **24** 1740010
[15] Seah S, Nimmrichter S and Scarani V 2018 Refrigeration beyond weak internal coupling *Phys. Rev. E* **98** 012131
[16] Naseem M T, Xuereb A and Müstecaplıoğlu O E 2018 Thermodynamic consistency of the optomechanical master equation *Phys. Rev. A* **98** 052123
[17] Cattaneo M, Giorgi G L, Maniscalco S and Zambrini R 2019 Local versus global master equation with common and separate baths: superiority of the global approach in partial secular approximation *New J. Phys.* **21** 113045
[18] Farina D, De Filippis G, Cataudella V, Polini M and Giovannetti V 2020 Going beyond local and global approaches for localized thermal dissipation *Phys. Rev. A* **102** 052208
[19] Elouard C, Herrera-Martí D, Esposito M and Auffèves A 2020 Thermodynamics of optical Bloch equations *New J. Phys.* **22** 103039
[20] Scali S, Anders J and Correa L A 2021 Local master equations bypass the secular approximation *Quantum* **5** 451
[21] Brunner N, Linden N, Popescu S and Skrzypczyk P 2012 Virtual qubits, virtual temperatures, and the foundations of thermodynamics *Phys. Rev. E* **85** 051117
[22] Mitchison M T 2019 Quantum thermal absorption machines: refrigerators, engines and clocks *Contemp. Phys.* **60** 164
[23] Levy A and Kosloff R 2014 The local approach to quantum transport may violate the second law of thermodynamics *Europhys. Lett.* **107** 20004
[24] Novotný T 2002 Investigation of apparent violation of the second law of thermodynamics in quantum transport studies *Europhys. Lett.* **59** 648
[25] Trushechkin A S and Volovich I V 2016 Perturbative treatment of inter-site couplings in the local description of open quantum networks *Europhys. Lett.* **113** 30005
[26] Dann R and Kosloff R 2020 Quantum thermo-dynamical construction for driven open quantum systems (arXiv:2012.07979)
[27] De Chiara G, Landi G, Hewgill A, Reid B, Ferraro A, Roncaglia A J and Antezza M 2018 Reconciliation of quantum local master equations with thermodynamics *New J. Phys.* **20** 113024
[28] Hewgill A, De Chiara G and Imparato A 2021 Quantum thermodynamically consistent local master equations *Phys. Rev. Res.* **3** 013165
[29] Kiršanskas G, Franckié M and Wacker A 2018 Phenomenological position and energy resolving Lindblad approach to quantum kinetics *Phys. Rev. B* **97** 035432
[30] Ptaszyński K and Esposito M 2019 Thermodynamics of quantum information flows *Phys. Rev. Lett.* **122** 150603
[31] Kleinherbers E, Szpak N, König J and Schützhold R 2020 Relaxation dynamics in a Hubbard dimer coupled to fermionic baths: phenomenological description and its microscopic foundation *Phys. Rev. B* **101** 125131
[32] Nathan F and Rudner M S 2020 Universal Lindblad equation for open quantum systems *Phys. Rev. B* **102** 115109
[33] Davidović D 2020 Completely positive, simple, and possibly highly accurate approximation of the Redfield equation *Quantum* **4** 326
[34] Schaller G and Brandes T 2008 Preservation of positivity by dynamical coarse graining *Phys. Rev. A* **78** 022106
[35] Majenz C, Albash T, Breuer H-P and Lidar D A 2013 Coarse graining can beat the rotating-wave approximation in quantum Markovian master equations *Phys. Rev. A* **88** 012103
[36] Cresser J D and Facer C 2017 Coarse-graining in the derivation of Markovian master equations and its significance in quantum thermodynamics (arXiv:1710.09939)
[37] Farina D and Giovannetti V 2019 Open-quantum-system dynamics: recovering positivity of the Redfield equation via the partial secular approximation *Phys. Rev. A* **100** 012107
[38] Mozgunov E and Lidar D 2020 Completely positive master equation for arbitrary driving and small level spacing *Quantum* **4** 227
[39] Schaller G and Ablaßmayer J 2020 Thermodynamics of the coarse-graining master equation *Entropy* **22** 525
[40] Becker T, Wu L-N and Eckardt A 2021 Lindbladian approximation beyond ultraweak coupling *Phys. Rev. E* **104** 014110
[41] Trushechkin A 2021 Unified Gorini–Kossakowski–Lindblad–Sudarshan quantum master equation beyond the secular approximation *Phys. Rev. A* **103** 062226
[42] Wang J-S, Agarwalla B K, Li H and Thingna J 2014 Nonequilibrium Green's function method for quantum thermal transport *Front. Phys.* **9** 673 Note the slightly different system-bath coupling
[43] Meir Y and Wingreen N S 1992 Landauer formula for the current through an interacting electron region *Phys. Rev. Lett.* **68** 2512
[44] Zhang W, Fisher T S and Mingo N 2007 The atomistic Green's function method: an efficient simulation approach for nanoscale phonon transport *Numer. Heat Transfer* B **51** 333
[45] Agarwalla B K and Segal D 2018 Assessing the validity of the thermodynamic uncertainty relation in quantum systems *Phys. Rev. B* **98** 155438
[46] Spohn H and Lebowitz J L 1978 Irreversible thermodynamics for quantum systems weakly coupled to thermal reservoirs *Adv. Chem. Phys.* **38** 109
[47] Brandner K and Seifert U 2016 Periodic thermodynamics of open quantum systems *Phys. Rev. E* **93** 062134

[48] Geva E, Rosenman E and Tannor D 2000 On the second-order corrections to the quantum canonical equilibrium density matrix *J. Chem. Phys.* **113** 1380
[49] SubaŞı Y, Fleming C H, Taylor J M and Hu B L 2012 Equilibrium states of open quantum systems in the strong coupling regime *Phys. Rev.* E **86** 061132
[50] Esposito M, Lindenberg K and van den Broeck C 2010 Entropy production as correlation between system and reservoir *New J. Phys.* **12** 013013
[51] Ptaszyński K and Esposito M 2019 Entropy production in open systems: the predominant role of intraenvironment correlations *Phys. Rev. Lett.* **123** 200603
[52] Strasberg P and Esposito M 2019 Non-Markovianity and negative entropy production rates *Phys. Rev.* E **99** 012120
[53] Esposito M, Harbola U and Mukamel S 2009 Nonequilibrium fluctuations, fluctuation theorems, and counting statistics in quantum systems *Rev. Mod. Phys.* **81** 1665
[54] Perarnau-Llobet M, Bäumer E, Hovhannisyan K V, Huber M and Acin A 2017 No-go theorem for the characterization of work fluctuations in coherent quantum systems *Phys. Rev. Lett.* **118** 070601
[55] Hofer P P 2017 Quasi-probability distributions for observables in dynamic systems *Quantum* **1** 32
[56] Kerremans T, Samuelsson P and Potts P P 2021 Probabilistically violating the first law of thermodynamics in a quantum heat engine (arXiv:2102.01395)
[57] Gasparinetti S, Solinas P, Braggio A and Sassetti M 2014 Heat-exchange statistics in driven open quantum systems *New J. Phys.* **16** 115001
[58] Silaev M, Heikkilä T T and Virtanen P 2014 Lindblad-equation approach for the full counting statistics of work and heat in driven quantum systems *Phys. Rev.* E **90** 022103
[59] Friedman H M, Agarwalla B K and Segal D 2018 Quantum energy exchange and refrigeration: a full-counting statistics approach *New J. Phys.* **20** 083026
[60] Kilgour M, Agarwalla B K and Segal D 2019 Path-integral methodology and simulations of quantum thermal transport: full counting statistics approach *J. Chem. Phys.* **150** 084111
[61] Kohler S, Dittrich T and Hänggi P 1997 Floquet–Markovian description of the parametrically driven, dissipative harmonic quantum oscillator *Phys. Rev.* E **55** 300
[62] Levy A, Alicki R and Kosloff R 2012 Quantum refrigerators and the third law of thermodynamics *Phys. Rev.* E **85** 061126
[63] Folland G B and Sitaram A 1997 The uncertainty principle: a mathematical survey *J. Fourier Anal. Appl.* **3** 207
[64] Tscherbul T V and Brumer P 2015 Partial secular Bloch–Redfield master equation for incoherent excitation of multilevel quantum systems *J. Chem. Phys.* **142** 104107
[65] Jeske J, Ing D J, Plenio M B, Huelga S F and Cole J H 2015 Bloch–Redfield equations for modeling light-harvesting complexes *J. Chem. Phys.* **142** 064104
[66] Spohn H 1978 Entropy production for quantum dynamical semigroups *J. Math. Phys.* **19** 1227
[67] Kosloff R 1984 A quantum mechanical open system as a model of a heat engine *J. Chem. Phys.* **80** 1625
[68] Hofer P P, Souquet J-R and Clerk A A 2016 Quantum heat engine based on photon-assisted Cooper pair tunneling *Phys. Rev.* B **93** 041418(R)
[69] Alicki R 1979 The quantum open system as a model of the heat engine *J. Phys. A: Math. Gen.* **12** L103
[70] Alicki R and Gelbwaser-Klimovsky D 2015 Non-equilibrium quantum heat machines *New J. Phys.* **17** 115012